COmmon Muon Proton Apparatus for Structure and Spectroscopy

Hard Exclusive production of π^0 at COMPASS

О.М.Кузнецов

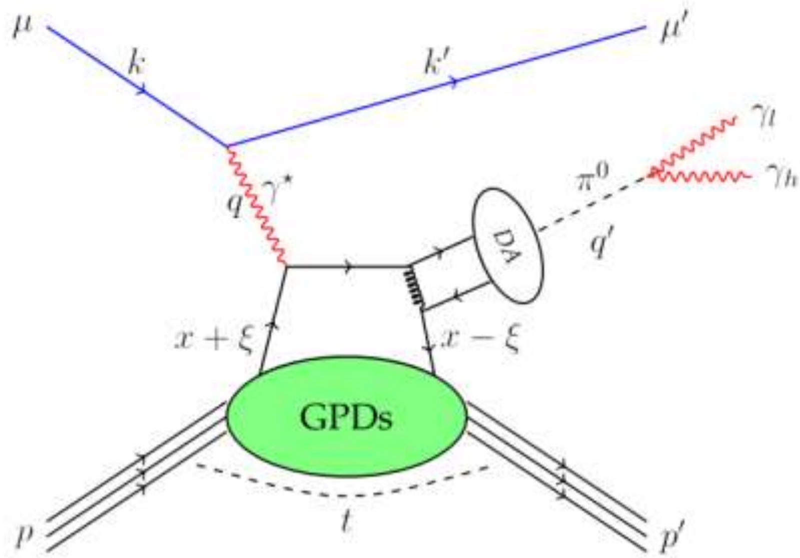

Definition of variables:
q . . . γ^* four-momentum
x . . . average longitudinal momentum fraction of initial and final parton (NOT accessible)
ξ . . . difference of longitudinal-momentum fraction between initial and final parton $\approx x_B/(2 - x_B)$
t . . . four-momentum transfer

$|t| \in (0.08, 0.64)\ (\mathrm{GeV}/c)^2$

DVCS vs. HEMP

Deeply Virtual Compton Scattering (DVCS): $\ell p \rightarrow \ell' \, p' \, \gamma$ (golden channel)

Hard Exclusive Meson Production (HEMP): $\ell p \rightarrow \ell' \, p'$ ... $\rho / \phi / J/\psi / \omega / \pi$

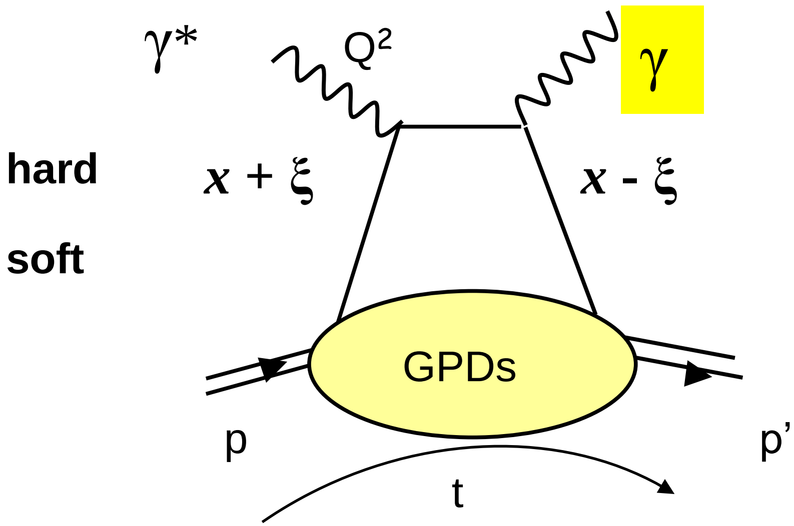

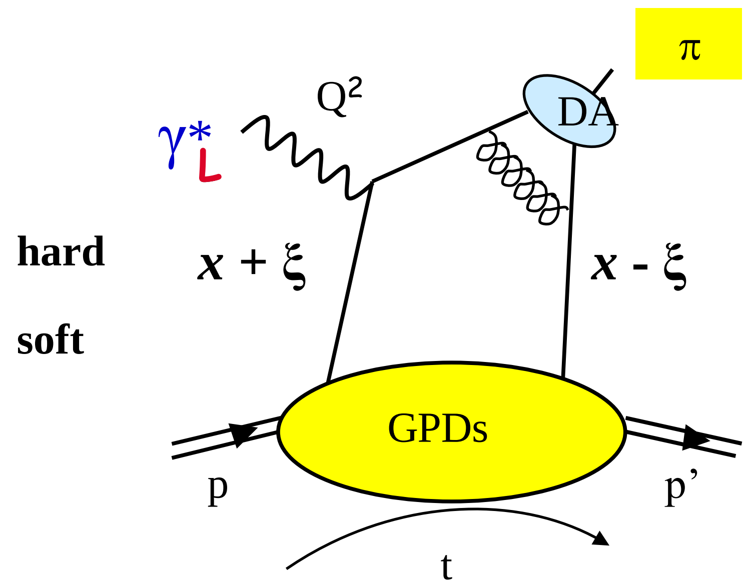

theoretically cleanest of the experimentaly accessible processes to measure GPDs

“Distribution Amplitude” should be taken in addition into account …. But gives possibility separate the flavors , access to GPDs gluons etc.

Exclusive π^0 production is the main source of background for DVCS process, while it provides important information on chiral-odd GPDs. The dedicated GPD program has started with a one month pilot run in 2012, followed by two full years of data taking in 2016-2017, using 160 GeV/c positive and negative muon beams, a liquid hydrogen target and new detectors such as a recoil proton detector and a large-angle electromagnetic calorimeter ECAL0.

Hard exclusive π^0 production on unpolarised protons and chiral-odd GPDs

Nucleon Polarisation	Quark Polarisation: Unpolarised (U)	Longitudinally polarised (L)	Tranversely polarised (T)
U	H		$\bar{E}_T$
L		$\tilde{H}$	$\tilde{E}_T$
T	E	$\tilde{E}$	$H_T, \tilde{H}_T$

$$\mu p \longrightarrow \mu' \pi^0 p'$$

μp cross-section can be reduced to γ*p due to the unpolarized proton target

$$\gamma^* p \longrightarrow \pi^0 p'$$

In general, hard exclusive π^0 is sensitive to the GPDs conserving the parton helicity $(\tilde{H},\ \tilde{E})$ and also to the parton helicity flip or to chiral-odd GPDs $(H_T \text{ and } \overline{E}_T)$, where $\bar{E}_T = 2\tilde{H}_T + E_T$

COMPASS experiment has excellent opportunity for studying Generalized Parton Distributions (GPD), through Deeply Virtual Compton Scattering (DVCS). DVCS is considered to be the theoretically cleanest of the experimentally accessible processes.

Exclusive <u>one single photon</u> production

$d\sigma \ \alpha \ |T_{BH}|^2 + |T_{DVCS}|^2$ + Interference Term

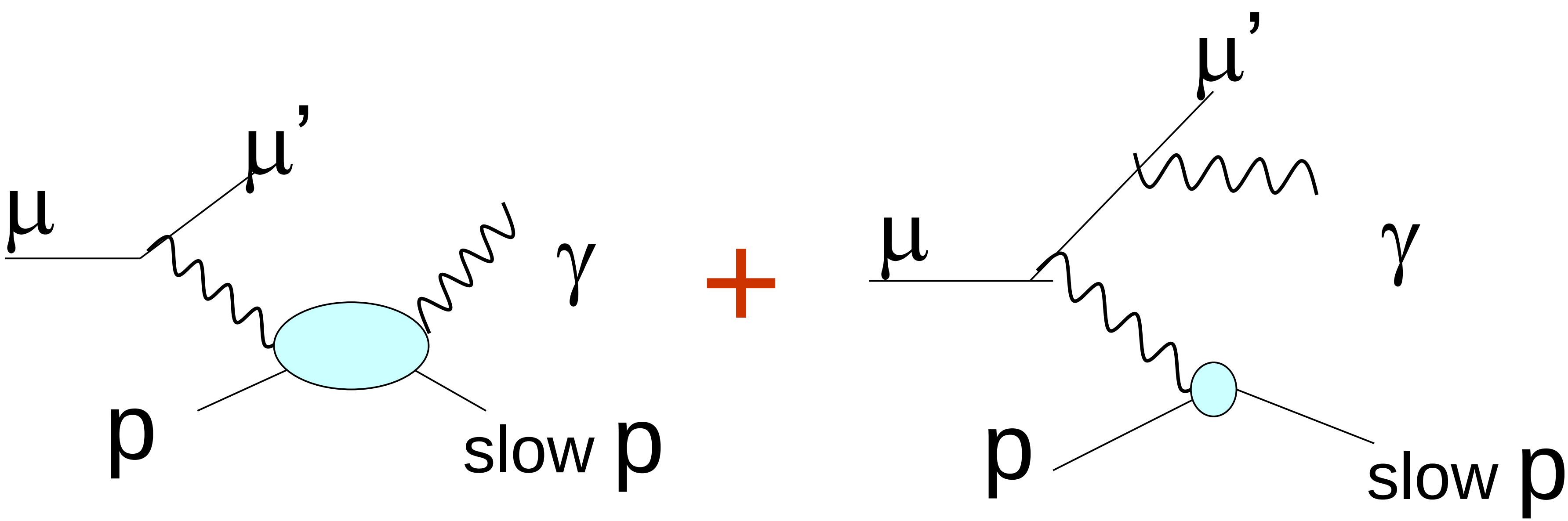

DVCS signal

DVCS/BH~1/10

Bethe Heitler signal

Exclusive single photon production $\ell p \rightarrow \ell' p' \gamma$

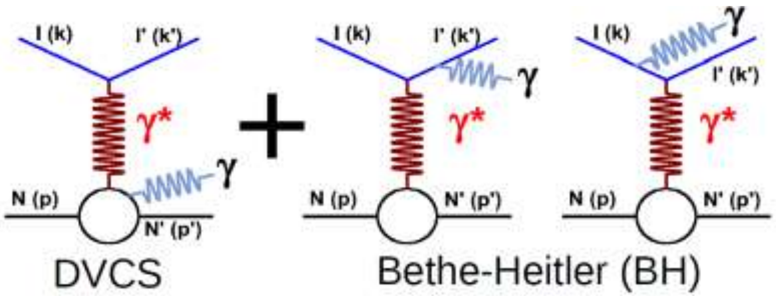

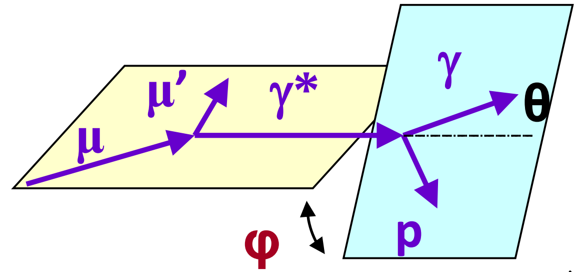

Known to 1 %

Monte-Carlo using set-up with ECAL1+ECAL2

$$d\sigma \propto |T^{DVCS}|^2 + Im(T^{DVCS}) \cdot T^{BH} + Re(T^{DVCS}) \cdot T^{BH} + |T^{BH}|^2$$

$0.005 < x_B < 0.01$

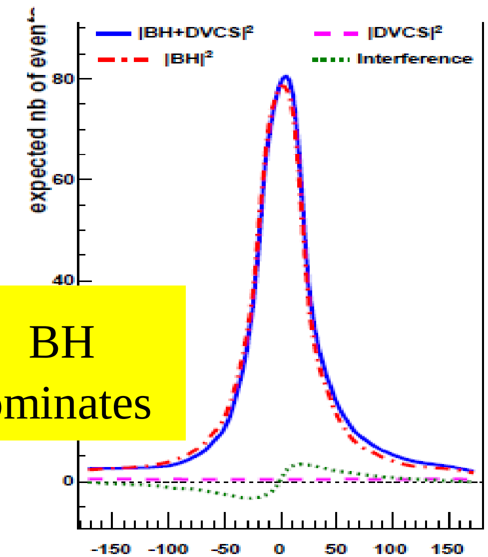

BH dominates

reference from almost pure Bethe-Heitler

$0.01 < x_B < 0.03$

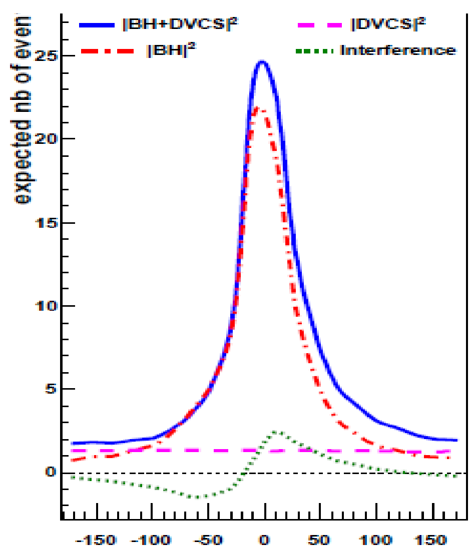

Study DVCS with:

$\Re(T^{DVCS})$ & $\Im(T^{DVCS})$

via $(d\sigma^{+\leftarrow} \pm d\sigma^{-\rightarrow})$

$0.03 < x_B$

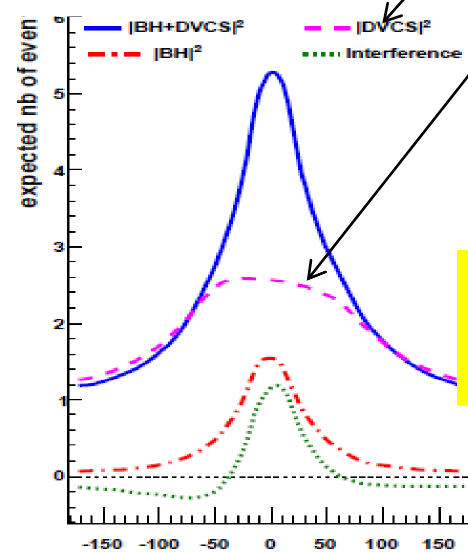

ECAL0 necessity

DVCS dominates

Transverse Imaging:

$d\sigma^{DVCS}/dt$

via $(d\sigma^{+\leftarrow} + d\sigma^{-\rightarrow})$

From PDFs to TMDs and GPDs

From Wigner distribution we can build ‘’mother distributions’’
$\mathcal{W}(x, b_\perp, k_\perp)$ → 3-dimensional nucleon structure
in momentum and configuration space:

PDF (x)

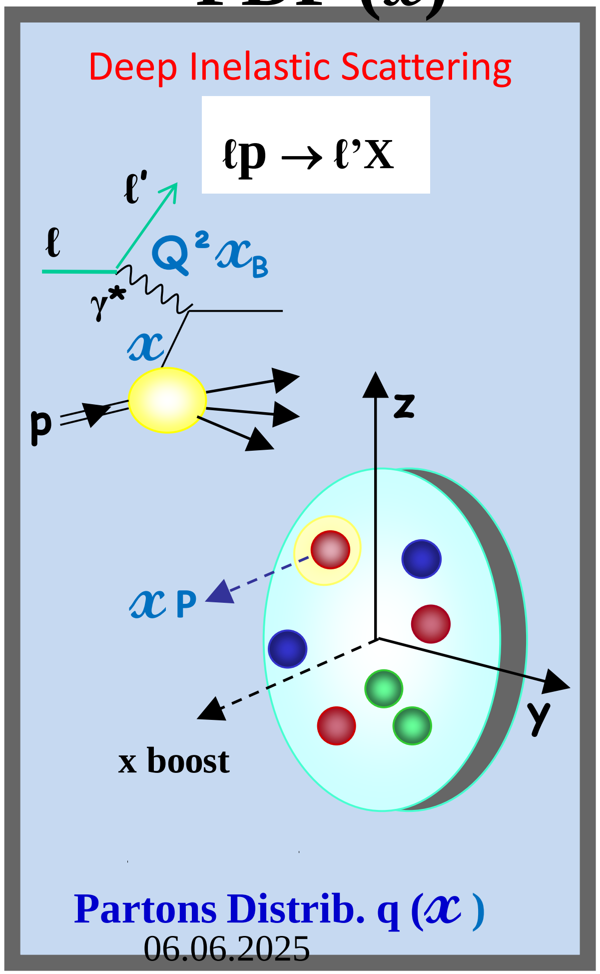

GPD $(x, b_\perp)$: Generalised Parton Distribution
(position in the transverse plane)

TMD $(x, k_\perp)$:Transverse Momentum Dependent
(momentum in the transv. plane)

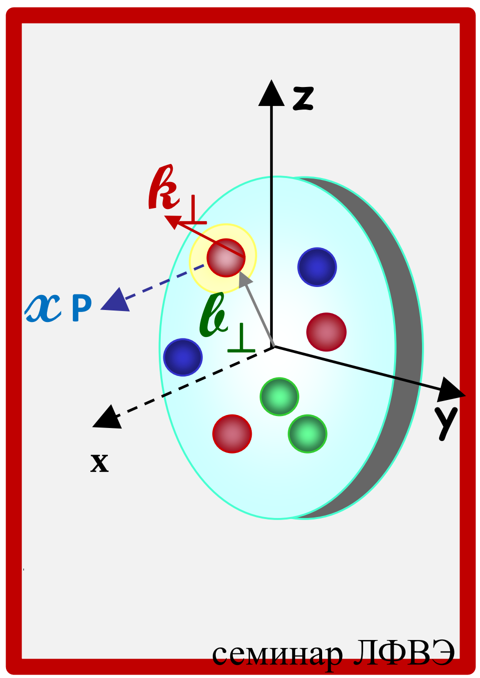

TMD accessible in SIDIS and DY

GPD in Exclusive reactions
DVCS and HEMP

The GPDs and TMDs provide
complementary
3-dimensional pictures of the nucleon.

GPDs and relations to the physical observables

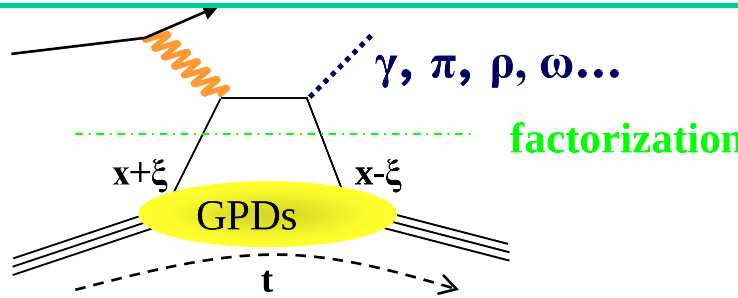

The observables are some integrals of GPDs over x

Dynamics of partons in the Nucleon Models: Parametrization

Fit of Parameters to the data

GPDs H, E, ...

8 GPDs for quarks and gluons:
$H, \widetilde{H}, E, \widetilde{E}, H_T, \widetilde{H}_T, E_T, \widetilde{E}_T$

Elastic Form Factors

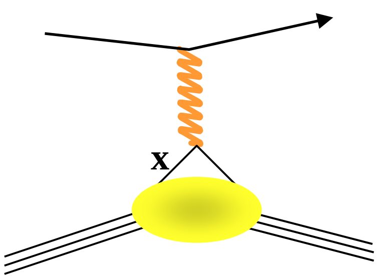

$$\int H(x,\xi,t)dx = F(t)$$

Ji's sum rule

$$2J_q = \int x(H+E)(x,\xi,0)dx$$

$$1/2 = \underbrace{1/2\ \Delta\Sigma + L_q}_{} + \Delta G + L_g$$

"ordinary" parton density

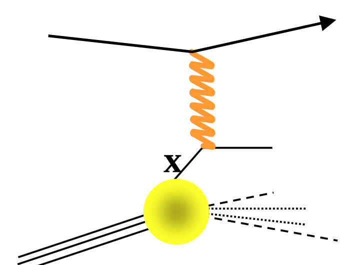

$$H(x,0,0) = q(x)$$

$$\widetilde{H}(x,0,0) = \Delta q(x)$$

- Proton spin sum rule: $\frac{1}{2} = \frac{1}{2}\Delta\Sigma + \Delta G + L_q + L_g$

EMC Collaboration, Nucl. Phys. B328 (1989) 180

COMPASS experiment in μp DIS: $\Delta\Sigma = 0.32 \pm 0.03$

COMPASS Collaboration: Phys. Lett. B 693 (2010)

COMPASS, RHIC results: $\Delta G = 0.2^{+0.06}_{-0.07}$

de Florian et al.Phys.Rev.Lett. 113 (2014), 012001

Missing component: $L_{q,g} = ?$ $\rightarrow$ GPDs provides access to the total angular momentum

COMPASS /AMBER тема 1085

Коллаж из слайдов Б.Парсамяна

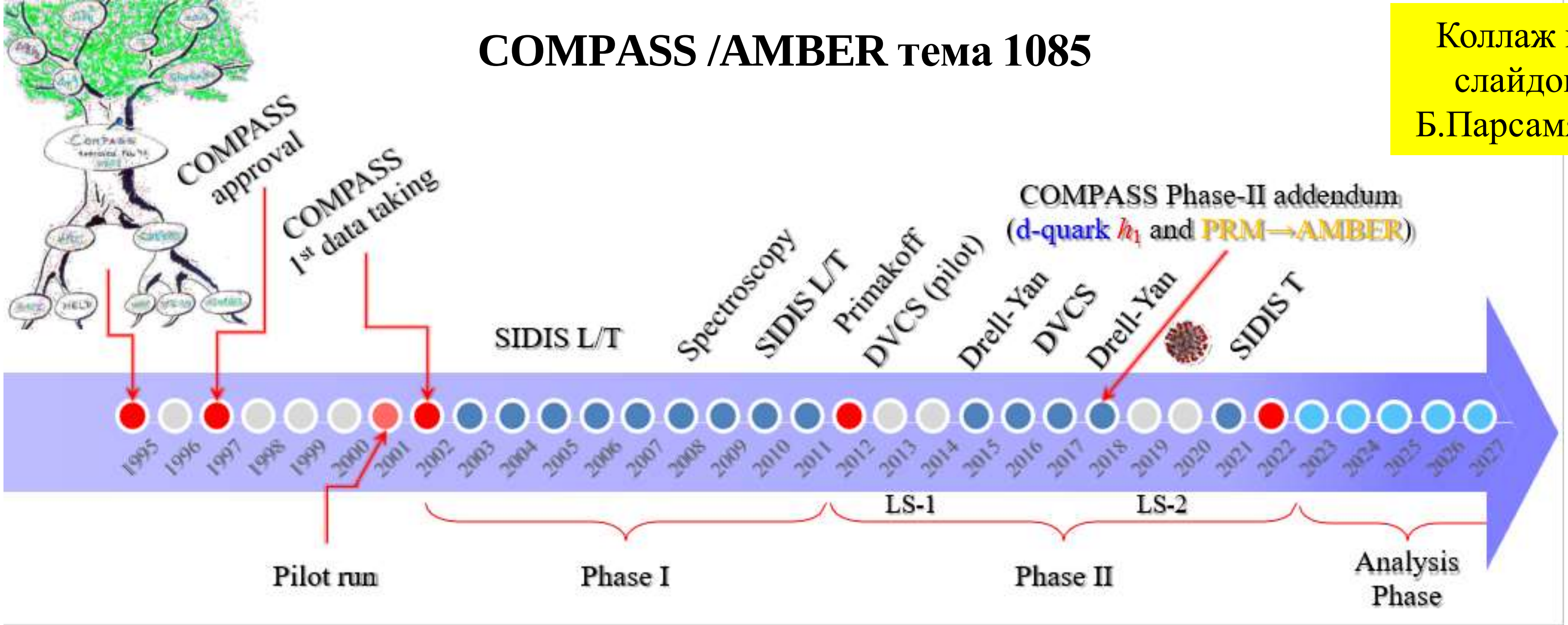

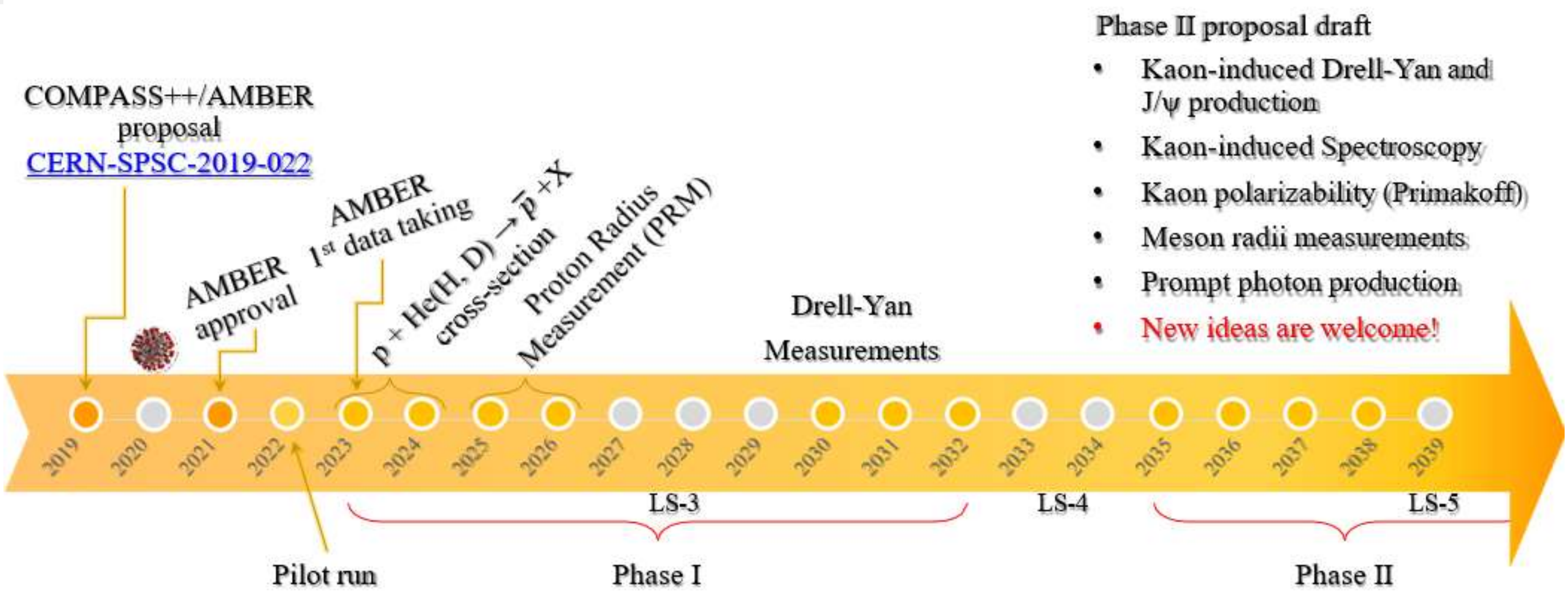

2002-2022 COMPASS data taking

2002-2004	DIS & SIDIS, μ^+-d, 160 GeV, **L & T polarized target**
2005	*CERN accelerator shutdown, increase of COMPASS acceptance*
2006	DIS & SIDIS, μ^+-d, 160 GeV, **L polarized target**
2007	DIS & SIDIS, μ^+-p, 160 GeV, **L & T polarized target**
2008-2009	Hadron spectroscopy & Primakoff reaction, **π/K/p** beam
2010	SIDIS, μ^+-p, 160 GeV, **T polarized target**
2011	DIS & SIDIS, μ^+-p, 200 GeV, **L polarized target**
2012	Primakoff reaction, **π/K/p** beam
2012 pilot run	DVCS/HEMP/SIDIS, μ^+ & μ^- -p, 160 GeV, **unpolarized target**
2013	*CERN accelerator shutdown, LS1*
2014-2015	Drell-Yan, π- -p, **T polarized target**
2016-2017	DVCS/HEMP/SIDIS, μ^+ & μ^- -p, 160 GeV, **unpolarized target**
2018	Drell-Yan, π- -p, **T polarized target**
2019-2020	*CERN accelerator shutdown, LS2*
2021-2022	SIDIS, μ^+-d, 160 GeV, **T polarized target**

COMPASS LEGACY

the work is not over

20 years have not been enough

as the CERN Director of Research says

> **“ it has not been easy to have COMPASS approved, it will not be easy to shut it down over the third millennium ”**

33 institutions from 15 countries: ~ 200 members

3 days ↓

2008 DVCS test run: a first observation of exclusive single-photon production.

10 days ↓

2009 DVCS test run: first estmation of pure DVCS, pure BH and DVCS-BH interference relative contributions

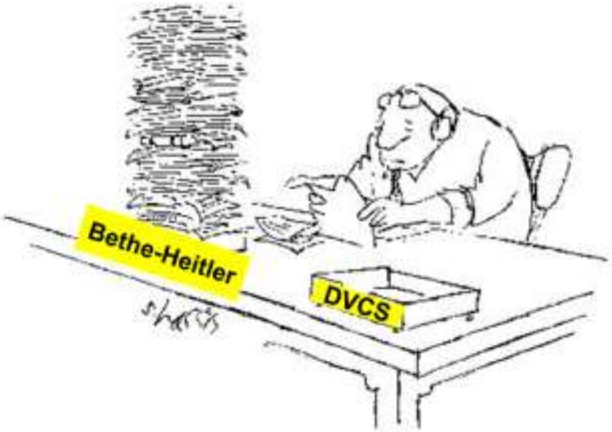

COMPASS spectrometer

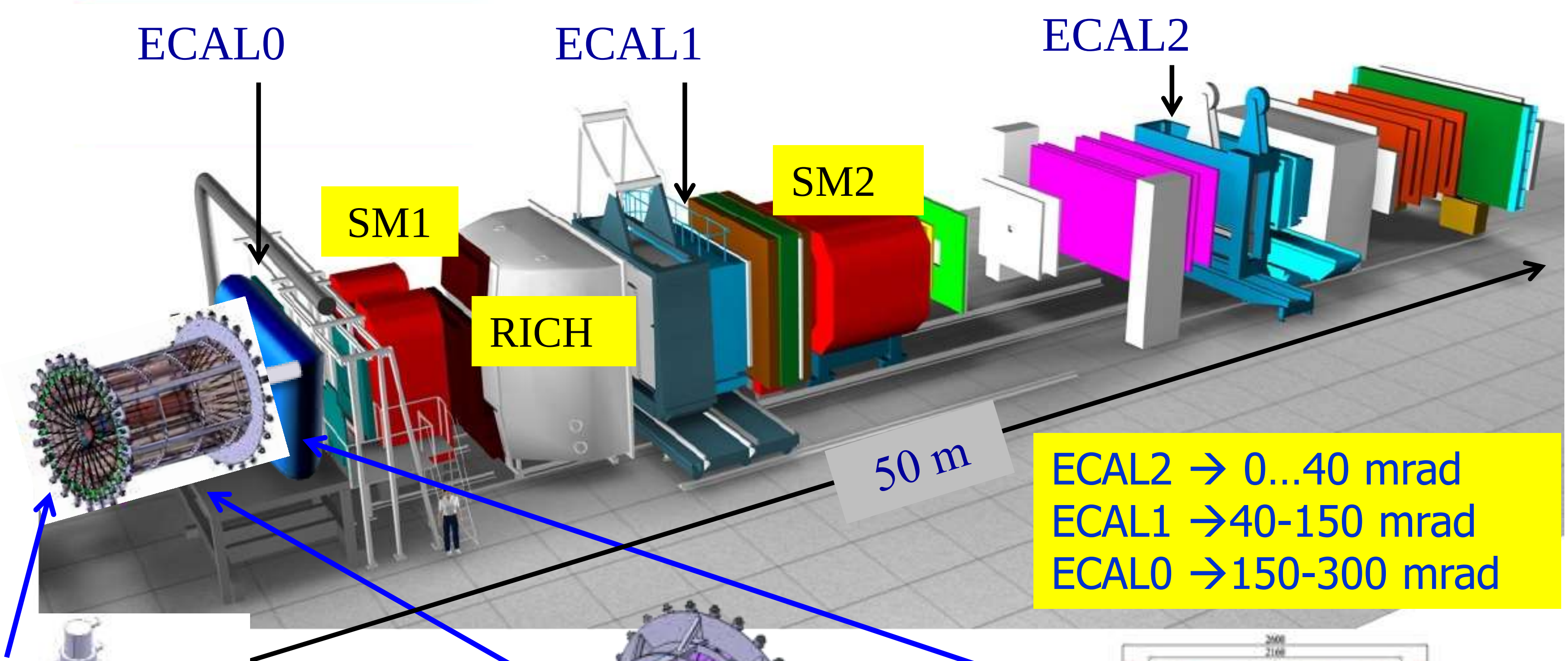

2.5 m long LH_2 target

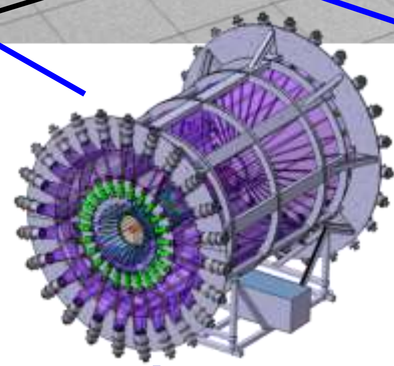

4.0 m longTime-Of-Flight detector: 24 inner and 24 outer slabs

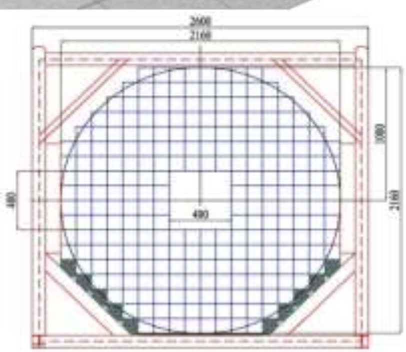

$2x2\ m^2$ electromagnetic calorimeter, ECAL0

Exclusive π^0 events selection

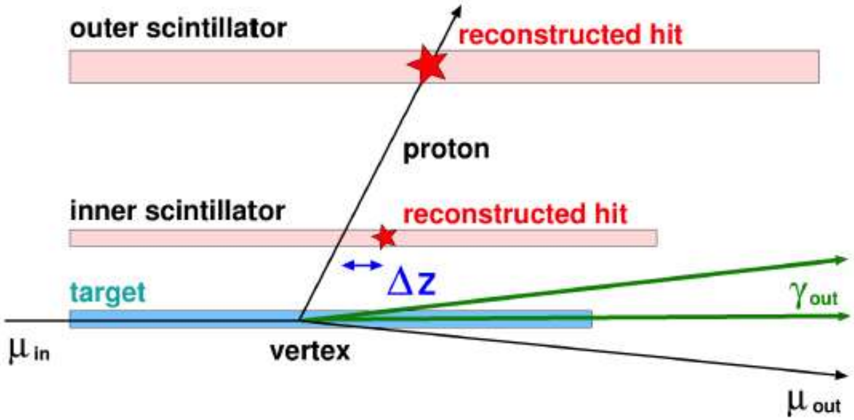

General selection in the phase-space

→
- 6.4 GeV < ν < 40 GeV
- 1 $(GeV/c)^2 < Q^2 < 8\ GeV/c)^2$
- 0.08 $(GeV/c)^2 < |t| < 0.64\ (GeV/c)^2$

→ Incoming and outcoming μ from the same/unique primary vertex

→ Two clusters in the ECAL0 , ECAL1 calorimeters

→ Identified proton in Time-of-flight detector CAMERA

Exclusivity variables

Transverse momentum constraint:

→ $\Delta p_T = p^p_{T,spect} - p^p_{T,recoil}$

→ $\Delta\varphi = \varphi^p_{spect} - \varphi^p_{recoil}$

Z coordinate of inner CAMERA ring:

→ $\Delta z = z^p_{spect} - z^p_{recoil}$

Energy-momentum conservation:

→ $M_X^2 = (p_{\mu,in} + p_p - p_{\mu,out} - p_{p'} - p_{\pi^0})^2$

$|\Delta\varphi| < 0.4$ rad,
$|\Delta p_T| < 0.3$ GeV/c ,
$|\Delta z| < 16$ cm,
$|M_X^2| < 0.3\ (GeV/c^2)^2$

Final selection

Invariant mass $M_{\gamma\gamma}$ cut

Kinematic fit

π^0 background to DVCS: complementarities of HEPGEN and LEPTO generators

HEPGEN predicts the possible background to exclusive single-γ events from exclusive π^0. However, in Real Data the semi-inclusive reactions enter in the game as the exclusive ones due to the imperfect overall energy resolution of the spectrometer.

LEPTO doesn't generate exclusive events but semi-inclusive ones. It is a general and flexible Monte Carlo generator to simulate complete lepton-nucleon scattering events and integrate cross sections. In contrast with HEPGEN Monte Carlo, LEPTO allows us to perform a more realistic comparison with Real Data. Moreover, it also permits to make predictions for the background for both the exclusive single-γ and the π^0 reactions

- "visible" π^0 (both γ detected, useful for MC normalization)
- "invisible" π^0 (one γ ``lost", only estimated with MC)

Measured and simulated $\Delta\phi$ and Δp_T

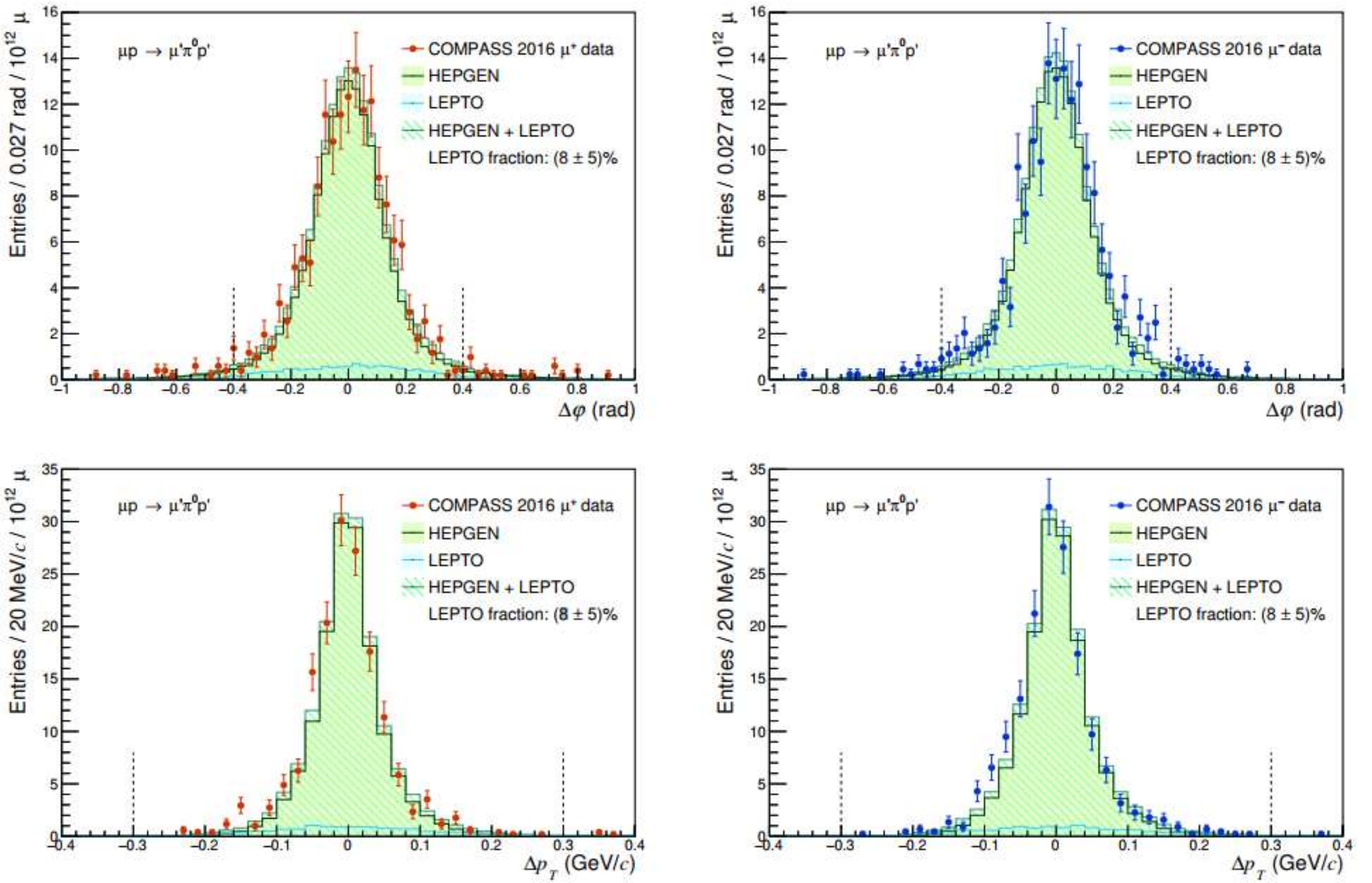

Measured and simulated 2 photon mass distributions

$$0.1061 < M_{\gamma\gamma}/(\mathrm{GeV}/c^2) < 0.1605$$

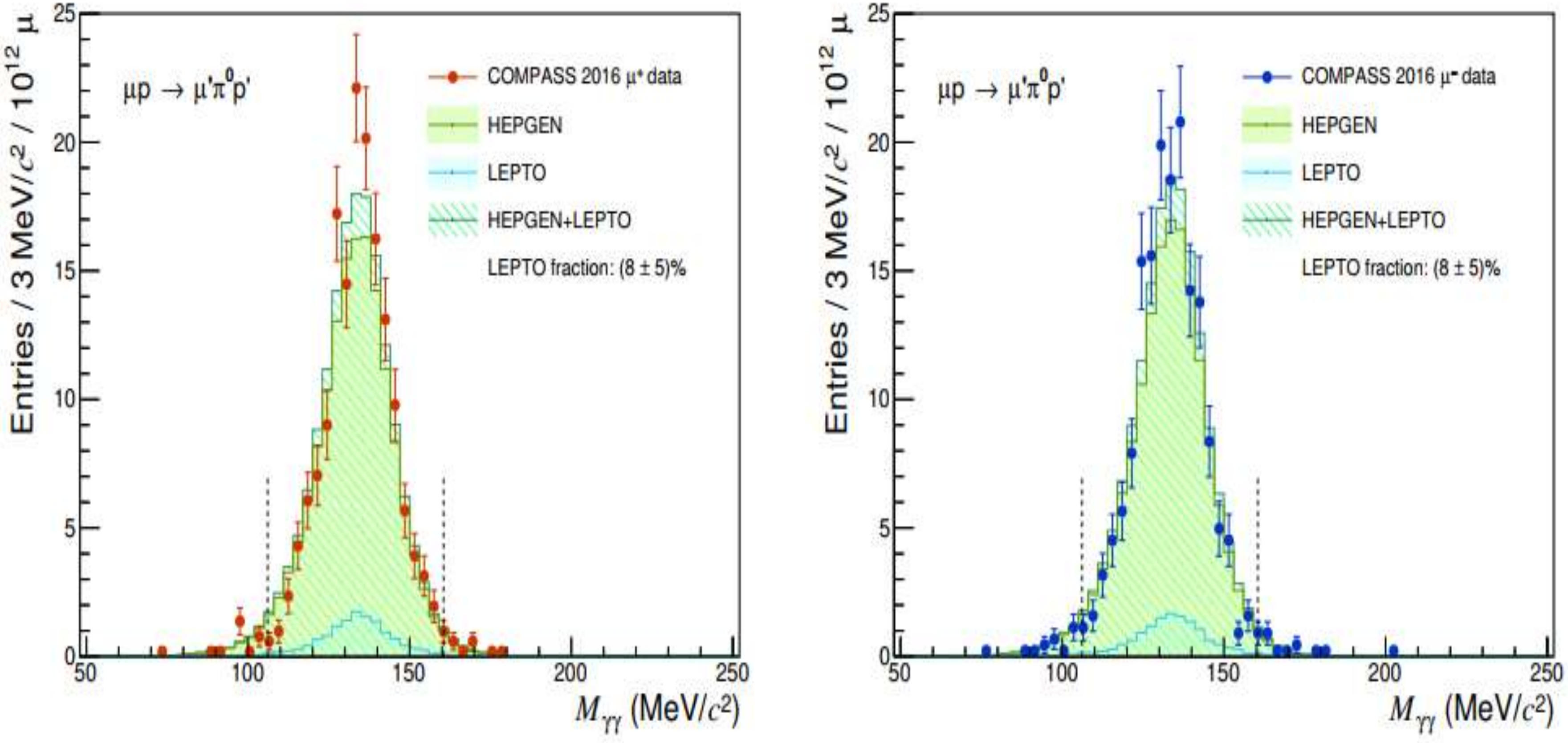

Thresholds of 2 GeV (2.5 GeV) for the higher-energy cluster and of 0.5 GeV (0.63 GeV) for the
lower-energy cluster in ECAL0 (ECAL1) are used.

Measured and simulated 2 photon mass distributions

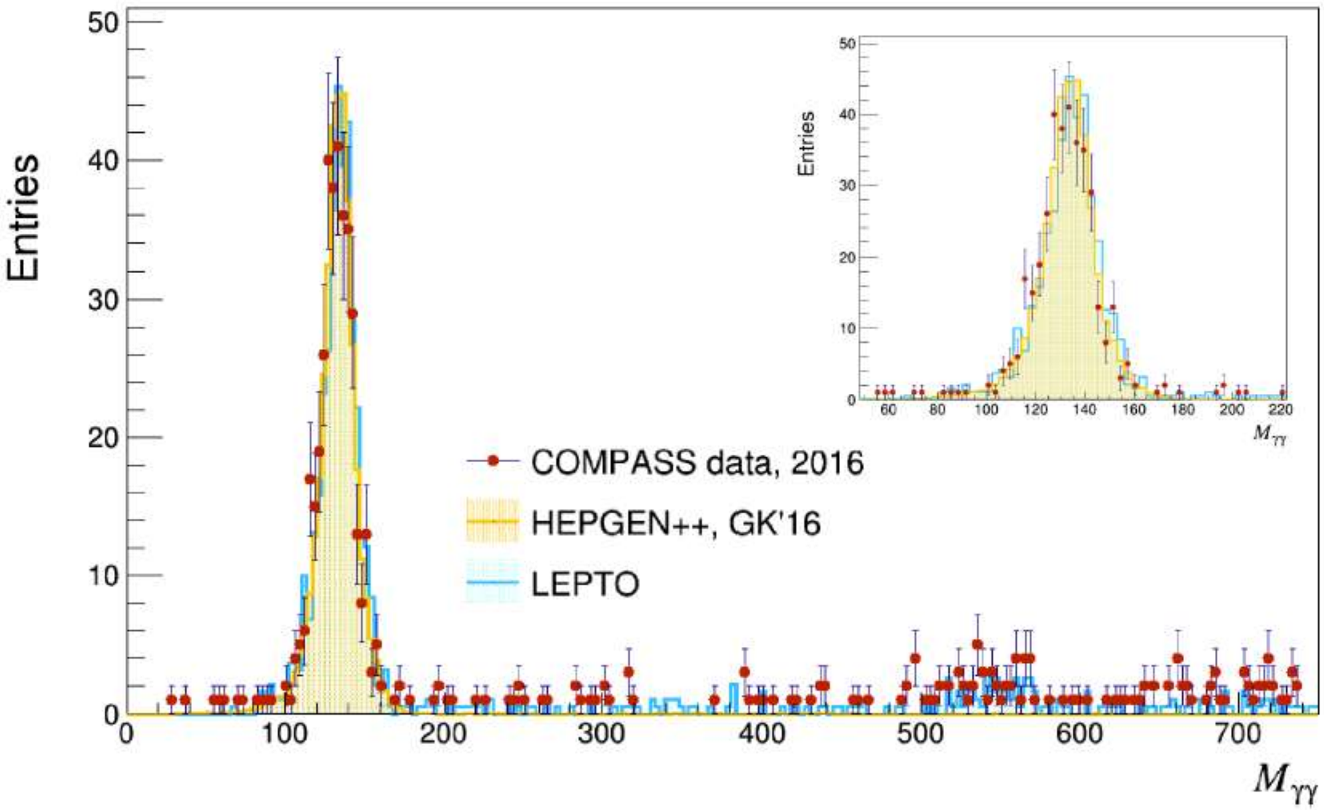

COMPASS η data

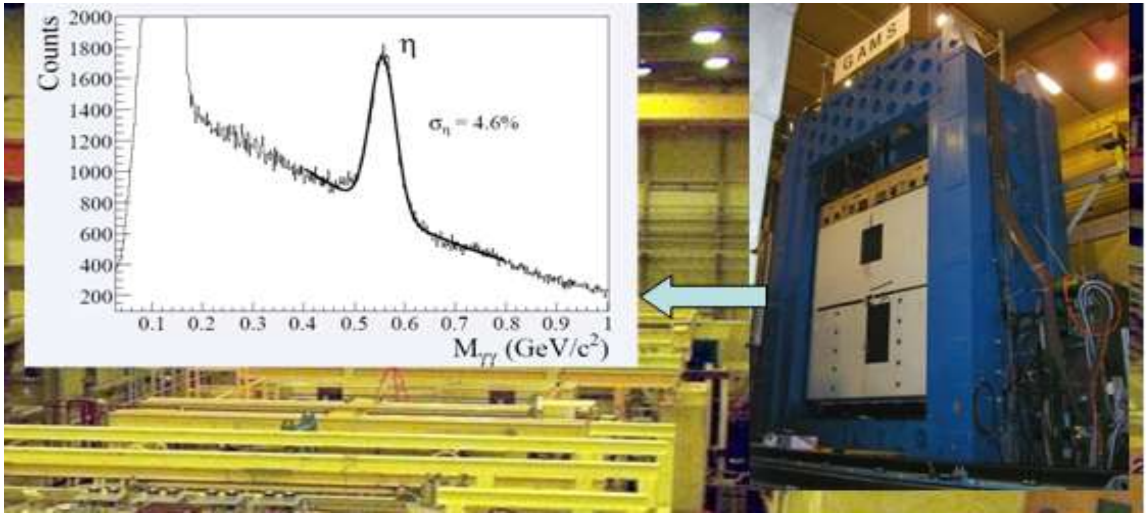

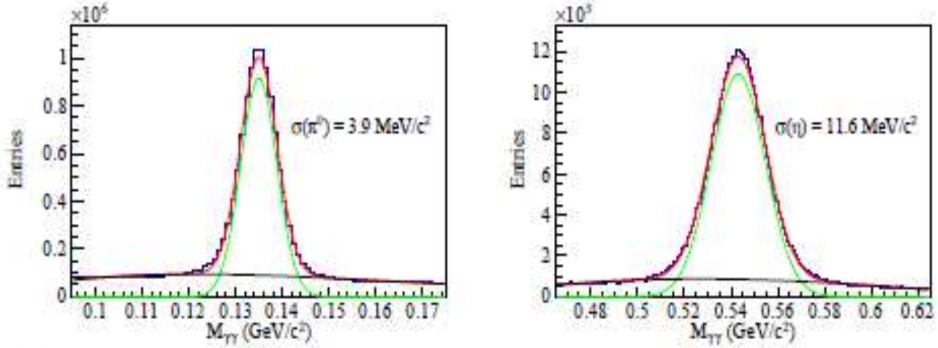

Fig. 98: Two-photon invariant mass distribution as measured in ECAL2, in the (left) π^0 mass region and (right) η mass region. The solid curves are fits to the signal and to the background. The values of the resolution achieved are indicated in each plot.

SIDIS background estimation

- Main background of π^0 production $\Rightarrow$ non-exclusive DIS processes
- 2 Monte Carlo simulations with the same π^0 selection criteria:
  - LEPTO for the non-exclusive background
  - HEPGEN++ shape of distributions of exclusive π^0 production (signal contribution)
- Search for best description of data fitting by mixture of both MC
- Both MC samples normalised to the experimental $M_{\gamma\gamma}$ distribution
- The ratio of background events r_{LEPTO} is determined by a fit on the exclusivity distributions

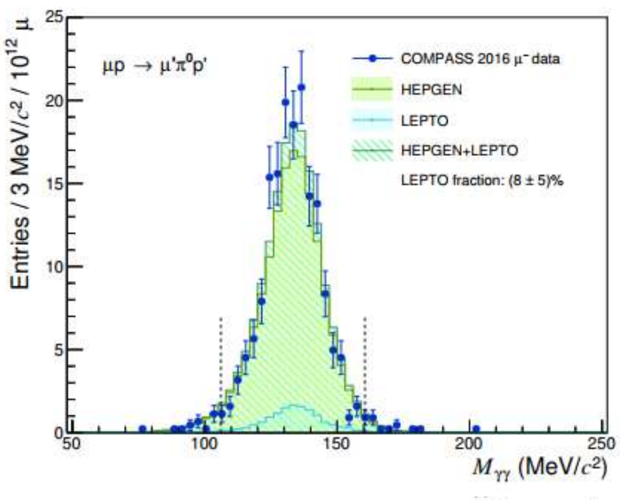

- Resulting fraction of non-exclusive background in data $\Rightarrow$ 8.5 +/- 5 %
- Background fit method is currently the main source of systematic uncertainty

Kinematically constrained fit for exclusive π^0

Measurement of exclusive processes at COMPASS is overconstrained $\rightarrow$ can be used to improve precision of kinematic quantities using kinematically constrained fit

Kinematic fit improves the resolution of the signal and lowers the background

It works in a principle of minimisation of least square function $\chi^2(\vec{k}) = (\vec{k}_{fit} - \vec{k})^T \hat{C}^{-1} (\vec{k}_{fit} - \vec{k})$, where $\vec{k}$ is a vector of measured quantities and $\hat{C}$ is their covariance matrix

Method used for the minimisation is Lagrange multipliers with constraints g_i:

$$L(\vec{k}, \vec{\alpha}) = \chi^2(\vec{k}) + 2\sum_{i=1}^{N} \alpha_i g_i$$

Constraints include momentum and energy conservation, common vertex for all tracks (except proton), constraints for final proton, and mass constraint

Hard exclusive π^0 production on unpolarised protons

Cross-section of the hard exclusive meson production, reduced to γ^*p, for the unpolarized target and polarized lepton beam

$$\frac{d^4\sigma_{\mu p}}{dQ^2 dt d\nu d\phi} = \Gamma \frac{d^2\sigma_{\gamma^* p}}{dt d\phi}$$

where $\Gamma = \Gamma(E_\mu, Q^2, \nu)$ is a transverse virtual-photon flux.

Spin independent cross-section of the hard exclusive meson production after averaging the two spin-dependent cross-sections looks following

$$\frac{d^2\sigma_{\gamma^* p}}{dt d\phi} = \frac{1}{2}\left(\frac{d^2\sigma^{\leftarrow}_{\gamma^* p}}{dt d\phi} + \frac{d^2\sigma^{\rightarrow}_{\gamma^* p}}{dt d\phi}\right) =$$

$$\frac{1}{2\pi}\left[\frac{d\sigma_T}{dt} + \epsilon\frac{d\sigma_L}{dt} + \epsilon\cos(2\phi)\frac{d\sigma_{TT}}{dt} + \sqrt{\epsilon(1+\epsilon)}\cos\phi\frac{d\sigma_{LT}}{dt}\right]$$

$\Rightarrow$ **study ϕ dependence**

After integration in ϕ:

$$\frac{d\sigma_T}{dt} + \epsilon\frac{d\sigma_L}{dt}$$

$\Rightarrow$ **study t dependence**

GPDs in exclusive π^0 production on unpolarised protons

$$\frac{d^2\sigma}{dt\,d\phi} = \frac{1}{2\pi}\left[\frac{d\sigma_T}{dt} + \varepsilon\frac{d\sigma_L}{dt} + \varepsilon\cos 2\phi\frac{d\sigma_{TT}}{dt} + \sqrt{2\varepsilon(1+\varepsilon)}\cos\phi\frac{d\sigma_{LT}}{dt}\right]$$

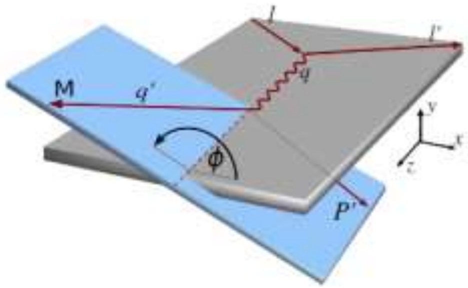

$$\frac{d\sigma_L}{dt} = \frac{4\pi\alpha}{k'}\frac{1}{Q^6}\left\{(1-\xi^2)\left|\langle\tilde{H}\rangle\right|^2 - 2\xi^2\mathrm{Re}\left[\langle\tilde{H}\rangle^*\langle\tilde{E}\rangle\right] - \frac{t'}{4m^2}\xi^2\left|\langle\tilde{E}\rangle\right|^2\right\}$$

leading twist

at JLAB only few% of $\frac{d\sigma_T}{dt}$

S. V. Goloskokov and P. Kroll, Eur. Phys. J. C **65**, 137 (2010), arXiv:0906.0460 [hep-ph]

S. V. Goloskokov and P. Kroll, Eur. Phys. J. A **47**, 112 (2011), arXiv:1106.4897 [hep-ph]

S. V. Goloskokov and P. Kroll, Private communications (2016).

def. $\bar{E}_T = 2\tilde{H}_T + E_T$

$$\frac{d\sigma_T}{dt} = \frac{4\pi\alpha}{2k'}\frac{\mu_\pi^2}{Q^8}\left[(1-\xi^2)\left|\langle H_T\rangle\right|^2 - \frac{t'}{8m^2}\left|\langle\bar{E}_T\rangle\right|^2\right]$$

phemenological Goloskokov&Kroll model in 2016 version considerably better fits COMPASS results after changing energy dependence of $\bar{E}_T$ which made the contribution from the transversely polarized γ* more important

$$\frac{\sigma_{LT}}{dt} = \frac{4\pi\alpha}{\sqrt{2}k'}\frac{\mu_\pi}{Q^7}\xi\sqrt{1-\xi^2}\frac{\sqrt{-t'}}{2m}\,\mathrm{Re}\left[\langle H_T\rangle^*\langle\tilde{E}\rangle\right]$$

$$\frac{\sigma_{TT}}{dt} = \frac{4\pi\alpha}{k'}\frac{\mu_\pi^2}{Q^8}\frac{t'}{16m^2}\left|\langle\bar{E}_T\rangle\right|^2$$

An impact of $\bar{E}_T$ should be visible in $\frac{\sigma_{TT}}{dt}$

and in a dip at small t' of $\frac{d\sigma_T}{dt}$

GPDs H and E for hard exclusive π^0 production

		Quark Polarisation		
		Unpolarised (U)	Longitudinally polarised (L)	Tranversely polarised (T)
Nucleon Polarisation	U	H		$\bar{E}_T$
	L		$\tilde{H}$	$\tilde{E}_T$
	T	E	$\tilde{E}$	$H_T, \tilde{H}_T$

- Sensitive to the GPDs
  - $\tilde{H}(x, \xi, t)$ and $\tilde{E}(x, \xi, t)$ - chiral-even (conserving the parton helicity)
  - $H_T(x, \xi, t)$ and $\bar{E}_T(x, \xi, t)$ - chiral-odd (parton helicity flip)

In general, hard exclusive π^0 is sensitive to the GPDs conserving the parton helicity $(\tilde{H}, \tilde{E})$ and also to the parton helicity flip or to chiral-odd GPDs $(H_T \text{ and } \overline{E}_T)$, where $\bar{E}_T = 2\tilde{H}_T + E_T$

GPDs in exclusive π^0 production on unpolarised protons

$$\frac{d^2\sigma}{dt\,d\phi} = \frac{1}{2\pi}\left[\frac{d\sigma_T}{dt} + \varepsilon\frac{d\sigma_L}{dt} + \varepsilon\cos 2\phi\frac{d\sigma_{TT}}{dt} + \sqrt{2\varepsilon(1+\varepsilon)}\cos\phi\frac{d\sigma_{LT}}{dt}\right]$$

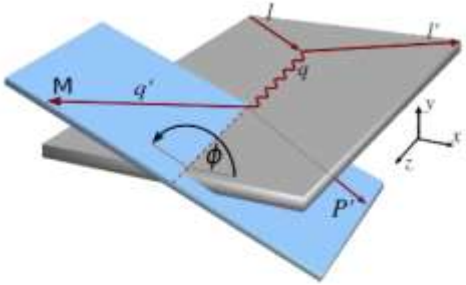

$$\frac{d\sigma_L}{dt} = \frac{4\pi\alpha}{k'}\frac{1}{Q^6}\left\{(1-\xi^2)\left|\langle\tilde{H}\rangle\right|^2 - 2\xi^2\mathrm{Re}\left[\langle\tilde{H}\rangle^*\langle\tilde{E}\rangle\right] - \frac{t'}{4m^2}\xi^2\left|\langle\tilde{E}\rangle\right|^2\right\}$$

leading twist

at JLAB only few% of $\frac{d\sigma_T}{dt}$

other contributions arise from coupling
of chiral-odd (quark helicity-flip) GPDs to twist-3 pion amplitude

def. $\bar{E}_T = 2\tilde{H}_T + E_T$

$$\frac{d\sigma_T}{dt} = \frac{4\pi\alpha}{2k'}\frac{\mu_\pi^2}{Q^8}\left[(1-\xi^2)\left|\langle H_T\rangle\right|^2 - \frac{t'}{8m^2}\left|\langle\bar{E}_T\rangle\right|^2\right]$$

$$\frac{\sigma_{LT}}{dt} = \frac{4\pi\alpha}{\sqrt{2}k'}\frac{\mu_\pi}{Q^7}\xi\sqrt{1-\xi^2}\frac{\sqrt{-t'}}{2m}\mathrm{Re}\left[\langle H_T\rangle^*\langle\tilde{E}\rangle\right]$$

$$\frac{\sigma_{TT}}{dt} = \frac{4\pi\alpha}{k'}\frac{\mu_\pi^2}{Q^8}\frac{t'}{16m^2}\left|\langle\bar{E}_T\rangle\right|^2$$

phemenological Goloskokov&Kroll model in 2016 version considerably better fits COMPASS results after changing energy dependence of $\bar{E}_T$

JLAB π^0 cross-sections are described fine as well.

An impact of $\bar{E}_T$ should be visible in $\frac{\sigma_{TT}}{dt}$

and in a dip at small t' of $\frac{d\sigma_T}{dt}$

the effect of H_T should be visible

Exclusive π^0 cross-section 2012 and 2016

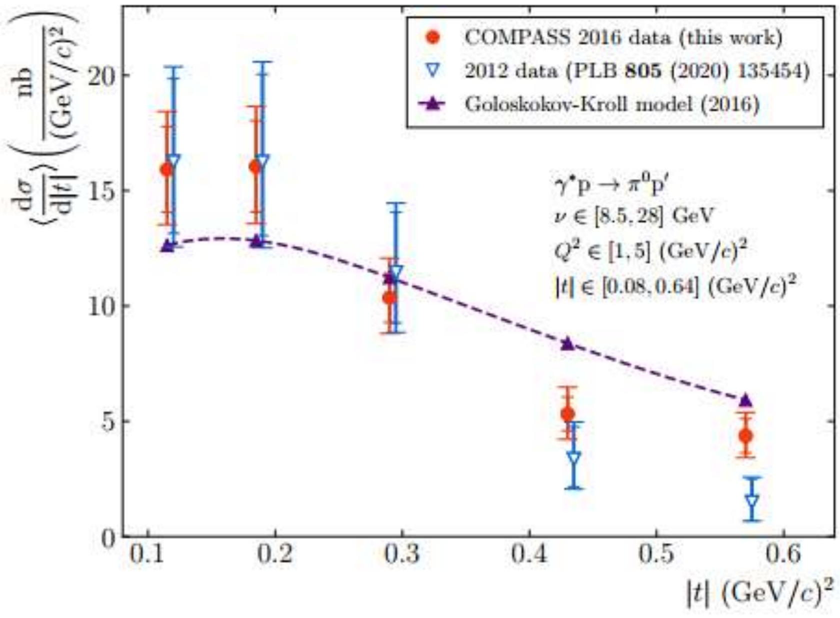

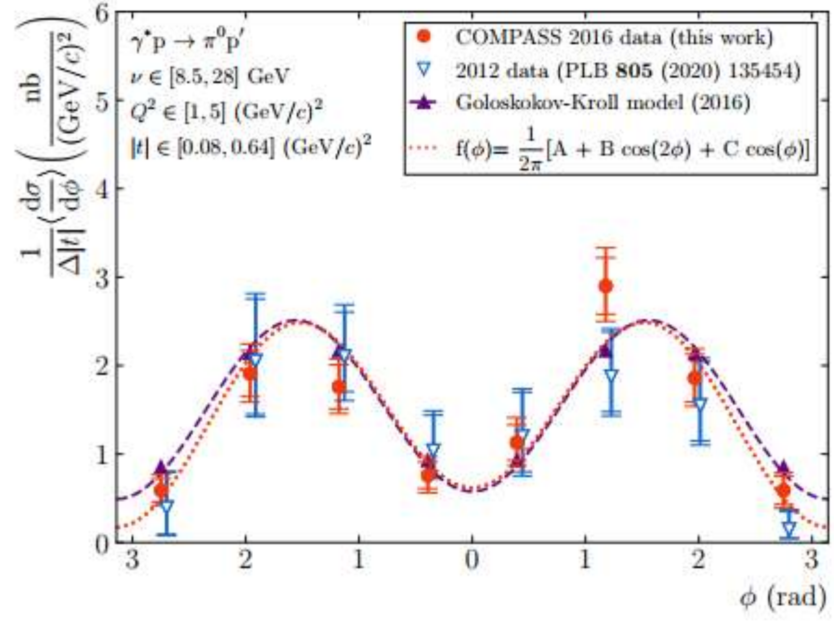

$$\frac{d^2\sigma}{dt\,d\phi} = \frac{1}{2\pi}\left[\frac{d\sigma_T}{dt} + \varepsilon\frac{d\sigma_L}{dt} + \varepsilon\cos 2\phi\frac{d\sigma_{TT}}{dt} + \sqrt{2\varepsilon(1+\varepsilon)}\cos\phi\frac{d\sigma_{LT}}{dt}\right]$$

	$\left\langle \frac{d\sigma_T}{d\lvert t\rvert} + \varepsilon\frac{d\sigma_L}{d\lvert t\rvert} \right\rangle$	$\left\langle \frac{d\sigma_{TT}}{d\lvert t\rvert} \right\rangle$	$\left\langle \frac{d\sigma_{LT}}{d\lvert t\rvert} \right\rangle$
2016 data	$9.0 \pm 0.5_{stat}\ {}^{+1.1}_{-1.0}\rvert_{sys}$	$-6.6 \pm 0.8_{stat}\ {}^{+0.5}_{-0.5}\rvert_{sys}$	$0.7 \pm 0.3_{stat}\ {}^{+0.4}_{-0.4}\rvert_{sys}$
2012 data	$8.1 \pm 0.9_{stat}\ {}^{+1.1}_{-1.0}\rvert_{sys}$	$-6.0 \pm 1.3_{stat}\ {}^{+0.7}_{-0.7}\rvert_{sys}$	$1.4 \pm 0.5_{stat}\ {}^{+0.3}_{-0.2}\rvert_{sys}$

Exclusive π^0 cross-section 2016 as a function of ϕ and t

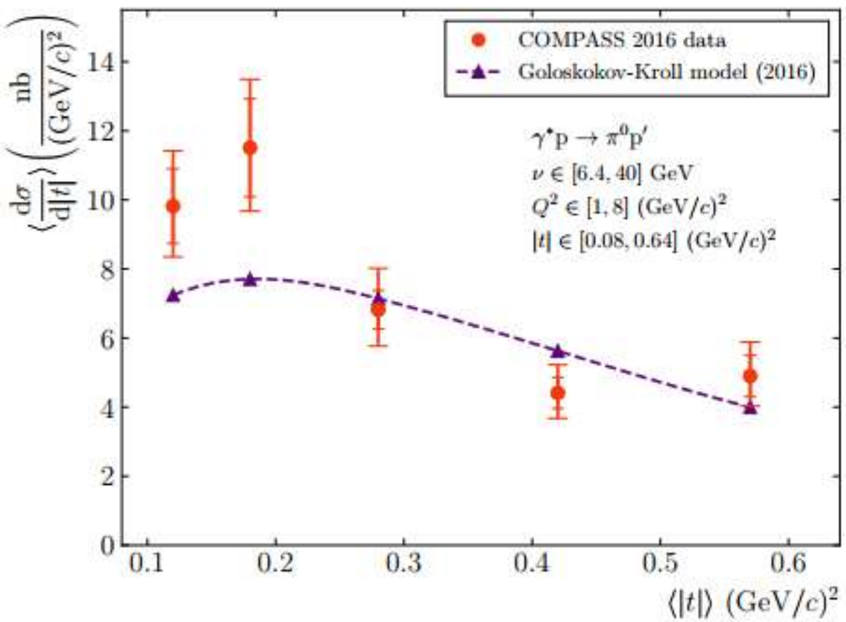

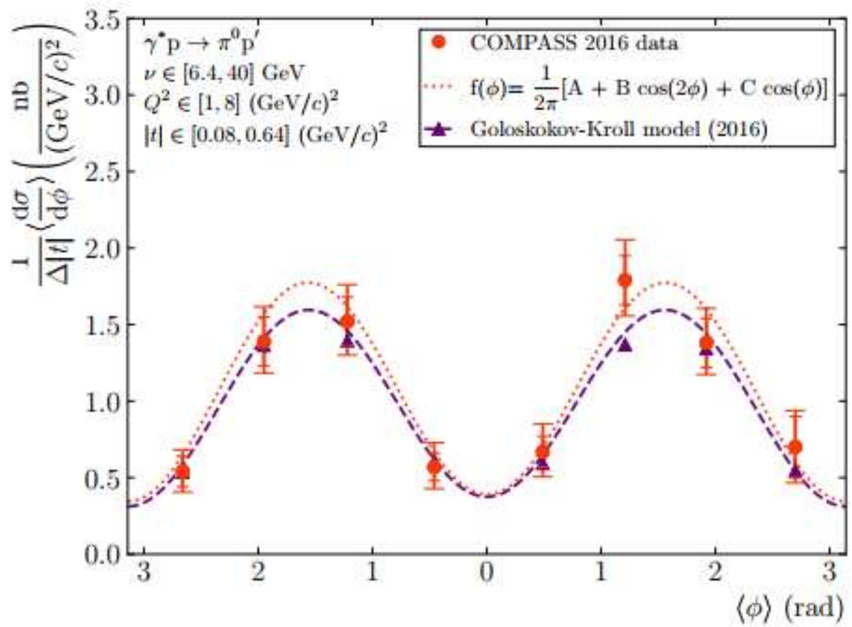

$\left\langle \frac{d\sigma_T}{d\|t\|} + \varepsilon \frac{d\sigma_L}{d\|t\|} \right\rangle$	$\left\langle \frac{d\sigma_{TT}}{d\|t\|} \right\rangle$	$\left\langle \frac{d\sigma_{LT}}{d\|t\|} \right\rangle$
$6.7 \pm 0.3_{\mathrm{stat}} {}^{+0.9}_{-0.8}\big\|_{\mathrm{sys}}$	$-4.4 \pm 0.5_{\mathrm{stat}} {}^{+0.3}_{-0.3}\big\|_{\mathrm{sys}}$	$0.1 \pm 0.2_{\mathrm{stat}} {}^{+0.1}_{-0.1}\big\|_{\mathrm{sys}}$

Exclusive π^0 cross-section as a function of ϕ and t in **ν/ Q^2 bins**

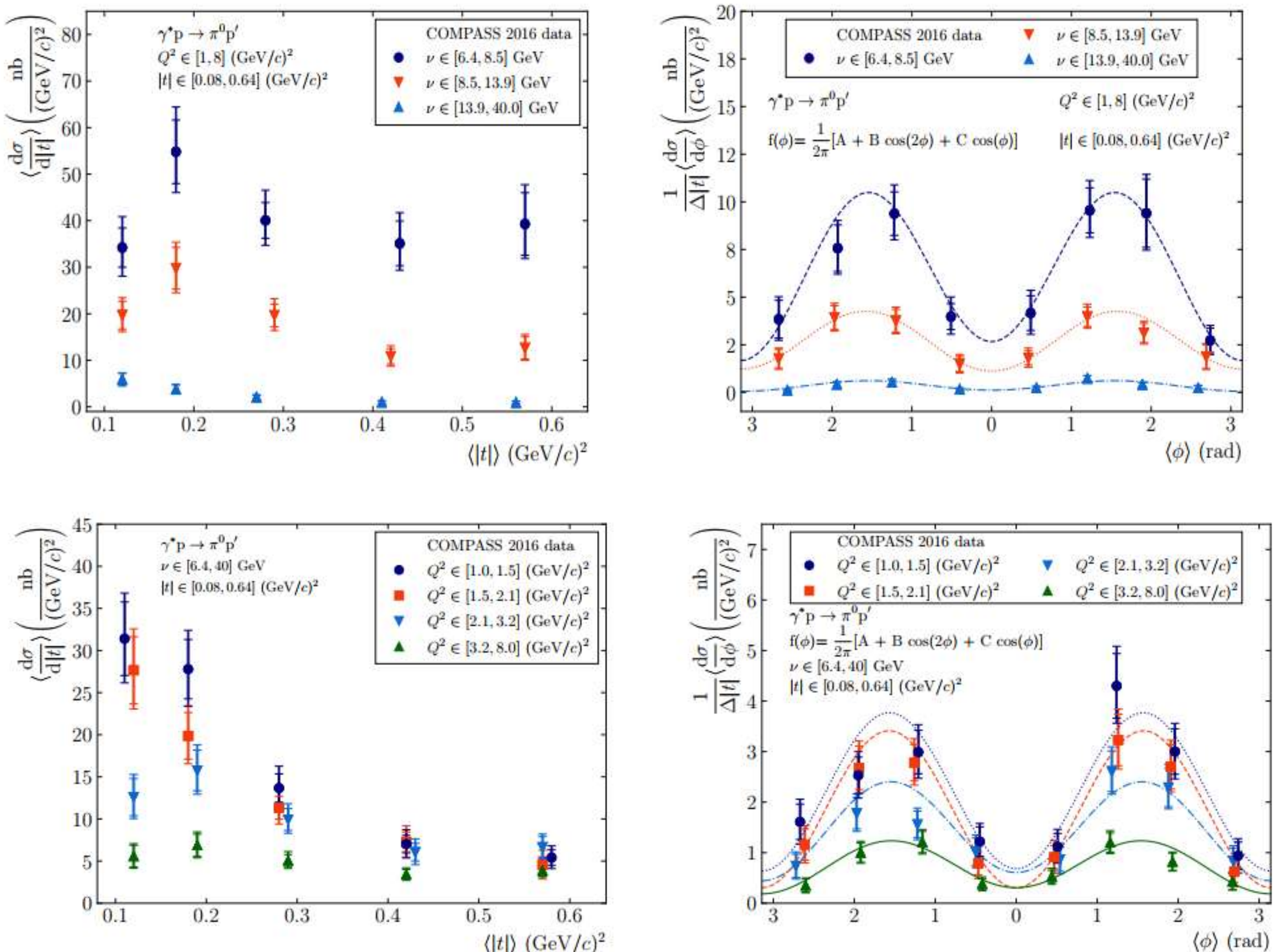

06.

$$\frac{d^2\sigma}{dt\,d\phi} = \frac{1}{2\pi}\left[\frac{d\sigma_T}{dt} + \varepsilon\frac{d\sigma_L}{dt} + \varepsilon\cos 2\phi\frac{d\sigma_{TT}}{dt} + \sqrt{2\varepsilon(1+\varepsilon)}\cos\phi\frac{d\sigma_{LT}}{dt}\right]$$

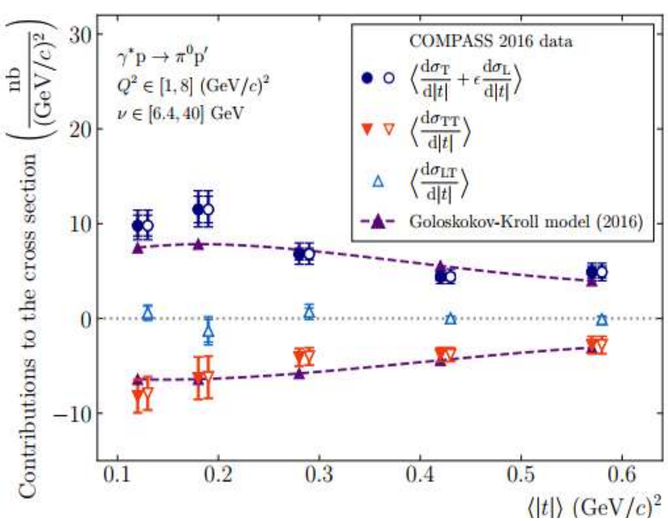

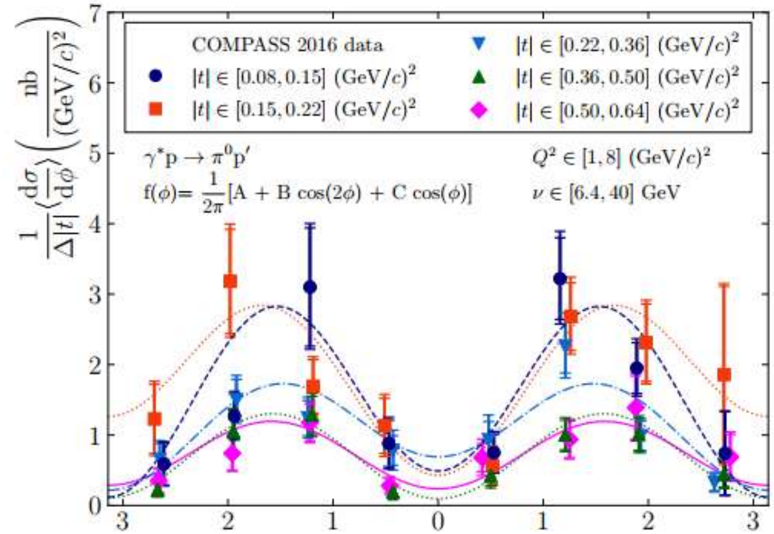

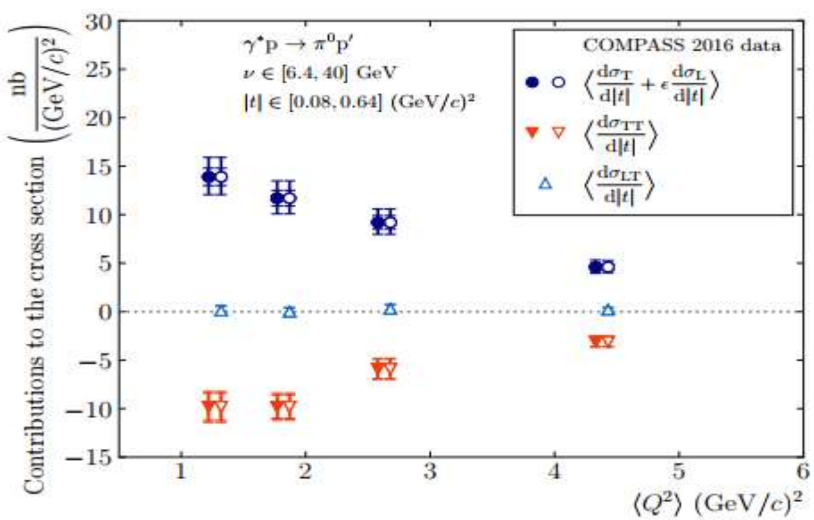

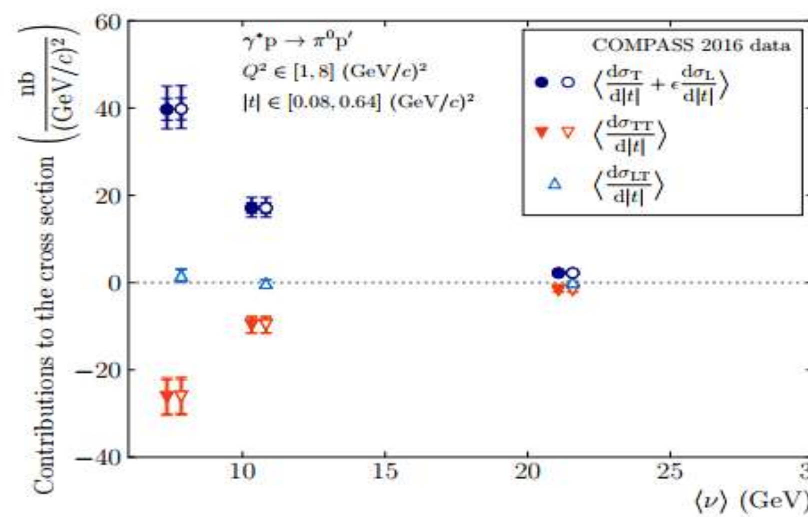

Table 2: Summary of the estimated relative systematic uncertainties on the measured $|t|$ and ϕ-dependent cross sections and on the extracted cross-section contributions $\frac{d\sigma_U}{dt} = \frac{d\sigma_T}{dt} + \varepsilon \frac{d\sigma_L}{dt}$ and $\frac{d\sigma_{TT}}{dt}$ in the full kinematic range. The values are given as a percentage. Note that the uni-directional uncertainty $\sigma_\uparrow$ ($\sigma_\downarrow$) has to be used with positive (negative) sign.

source	$\sigma^t_\uparrow$	$\sigma^t_\downarrow$	$\sigma^\phi_\uparrow$	$\sigma^\phi_\downarrow$	$\sigma_{U\uparrow}$	$\sigma_{U\downarrow}$	$\sigma_{TT\uparrow}$	$\sigma_{TT\downarrow}$
μ^+ flux	2	2	2	2	2	2	2	2
μ^- flux	2	2	2	2	2	2	2	2
acceptance	4	4	4	4	4	4	4	4
ECAL0 threshold	5 – 7	1	4 – 8	1	5	1	4	1
ECAL1 threshold	1 – 2	1	1 – 3	1	1	1	1	1
χ^2 of kinematic fit	3	5	2.0 – 5.6	4.0 – 8.8	3	5	3	4
LEPTO background	6 – 10	6 – 10	6 – 16	6 – 16	8.3	8.3	1	1
LEPTO normalisation	2 – 3	2 – 3	2 – 5	2 – 5	2.6	2.6	2	2
ω background	0	1.5 – 2.7	0	1.4 – 5.7	0	2.4	0	2.4
radiative corrections	6	3	6.3	3.6	6	3	2	2
Σ	12 – 16	10.1 – 13.1	11.6 – 22.4	9.6 – 20.1	13.3	11.7	7.7	7.1

Exclusive π^0 : COMPASS acceptance after ECAL0 installation in 2016

The cross section is determined presently in the same phase space as for the 2012 data analysis:

- $8.5\ \text{GeV} < \nu < 28\ \text{GeV}$
- $1\ (\text{GeV/c})^2 < Q^2 < 5\ (\text{GeV/c})^2$
- $0.08\ (\text{GeV/c})^2 < |t| < 0.64\ (\text{GeV/c})^2$

For the acceptance determination, the HEPGen-π0 MC simulation is used.

4D acceptance in bins of φ_{π^0}, ν, $|t|$, Q^2

- 5 bins in |t| with binning [0.08, 0.15], [0.15 0.22], [0.22 0.36], [0.36 0.5] [0.5 0.64] $(\text{GeV/c})^2$,
- 8 bins in ϕ equally spaced from $-\pi$ to $+\pi$
- 4 bins in Q^2 with binning [1, 1.5], [1.5 2.24], [2.24 3.34], [3.34 5] $(\text{GeV/c})^2$,
- 4 bins in ν with binning [8.5, 11.45], [11.45 15.43], [15.43 20.78], [20.78 28] (GeV).

Exclusive π^0 production: COMPASS acceptance |t| averaged

4D acceptance in bins of ϕ_{π^0}, ν, $|t|$, Q^2
figure shows 3D projection, as a function of ϕ_{π^0}

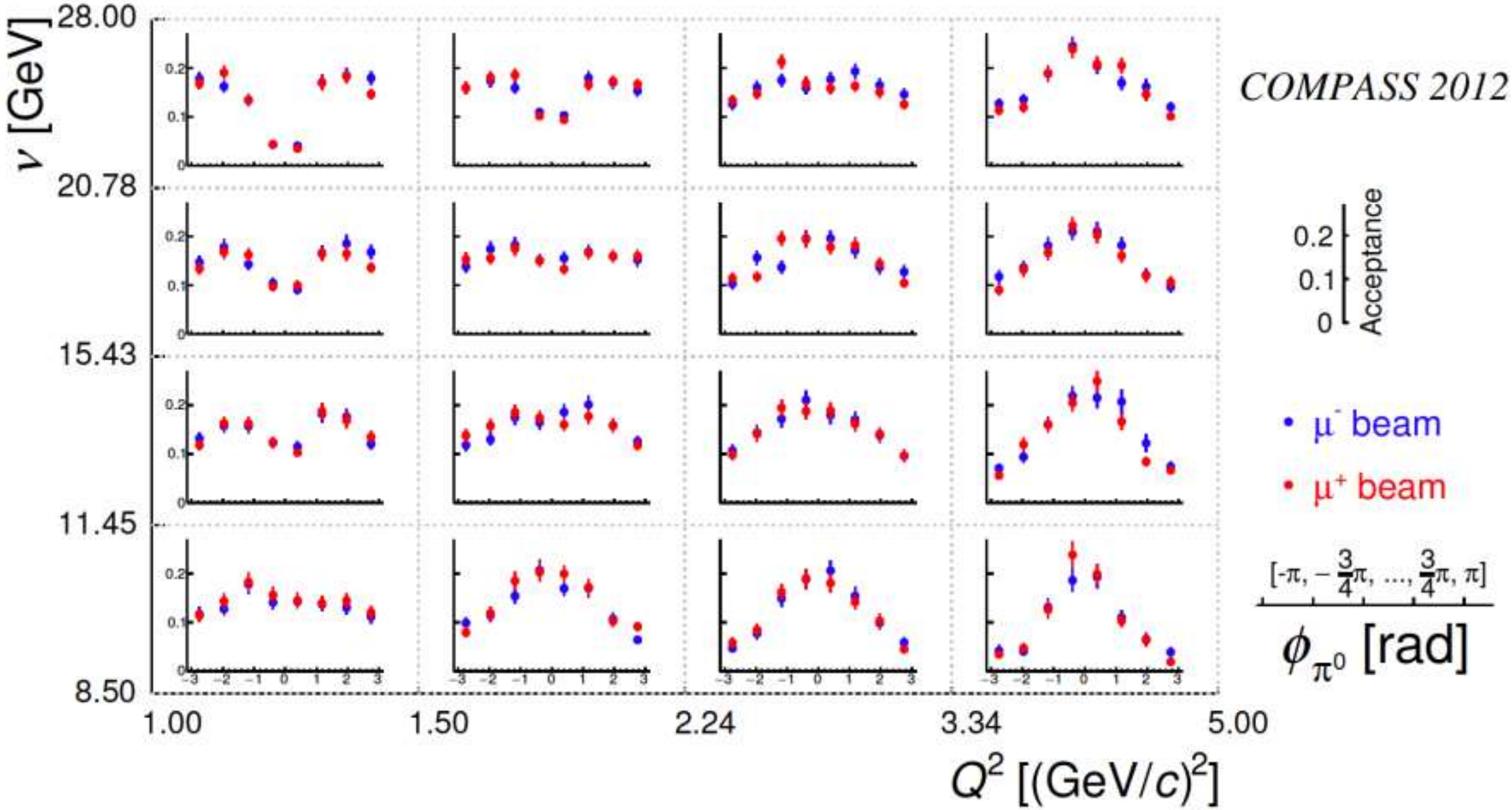

Exclusive π^0 production: COMPASS acceptance |t| averaged

4D acceptance in bins of ϕ_{π^0}, ν, $|t|$, Q^2
figure shows 3D projection, as a function of ϕ_{π^0}

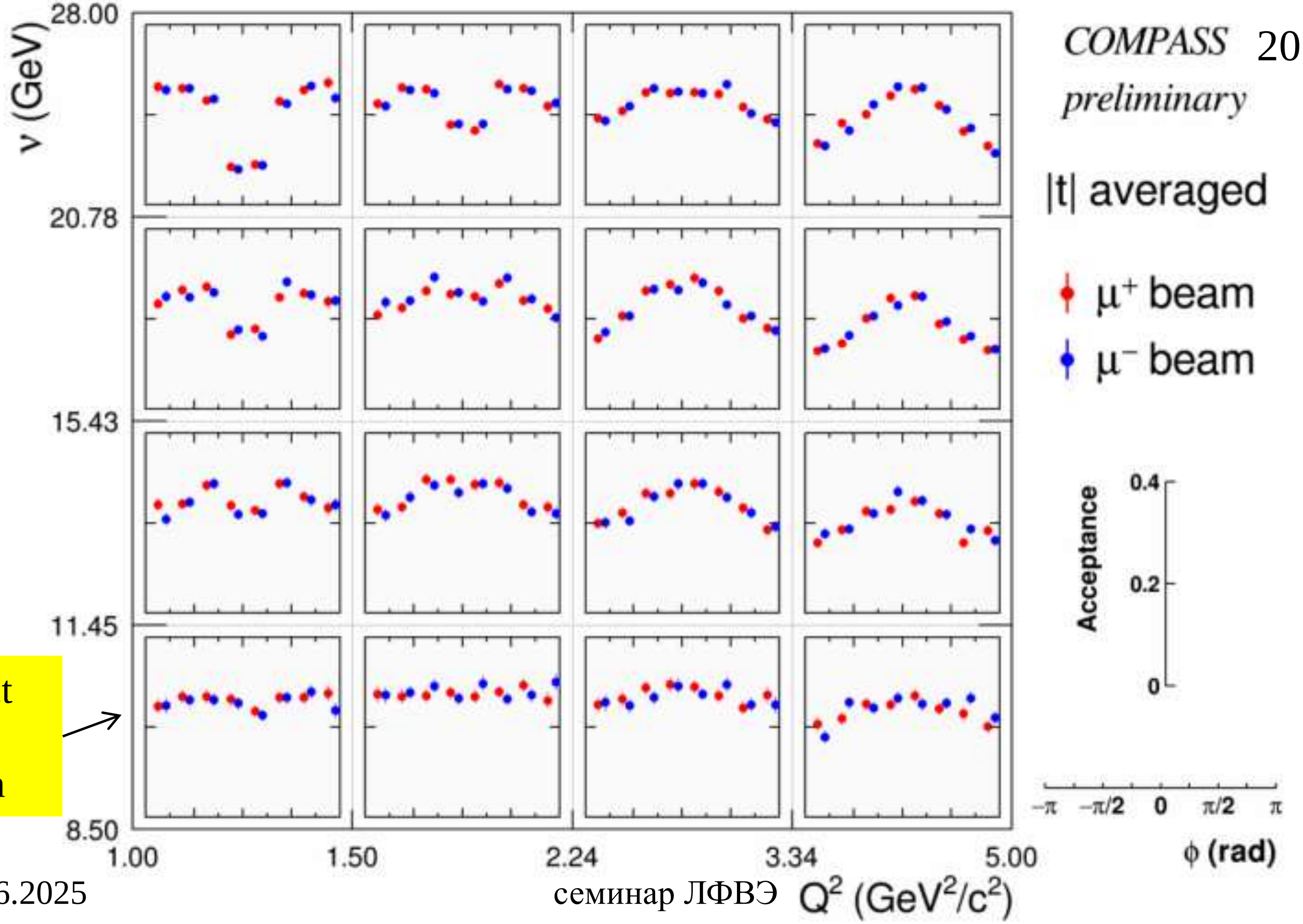

2016

Clear effect of ECAL0 installation

Summary

➔The differential virtual-photon proton cross sections are extracted from the 2016 data (~1500 events) as a function of the squared four-momentum transfer t, and of the azimuthal angle ϕ between the scattering plane and the π^0 production plane.

➔The average differential cross sections from the 2016 data are compared to the published results of the 2012 data and there are no significant difference is observed.

➔A slightly different t-shape is seen in 2016 data (as in 2012 one) with respect to GK2016 model prediction, which however can be reduced in the GK2016 + an updated model with another energy dependence of $\bar{E}_T$

➔From the results we observe a large contribution of σ_{TT} and a negligible contribution of σ_{LT} .
This supports the expectation of the exclusive π^0cross section to be dominated by transverse polarized virtual photon, which indicates a significant effect of the chiral-odd GPD

➔Total statistics 2017+2016 data is estimated to be 10 times higher than the 2012 one
➔Input for constraining phenomenological models.

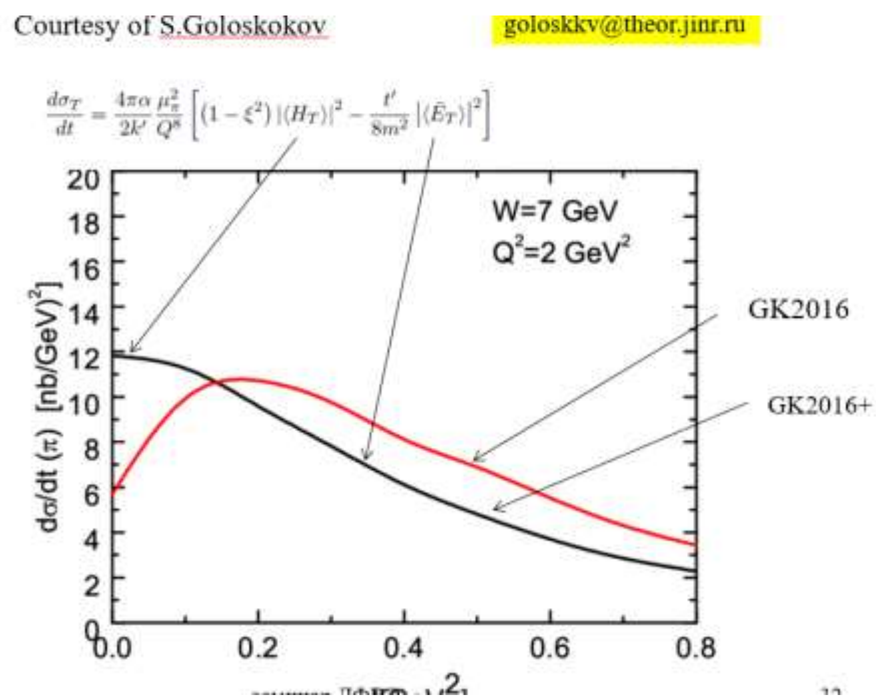

First collaboration meeting

CLAS paper: PHYSICAL REVIEW C **95, 035202 (2017)**

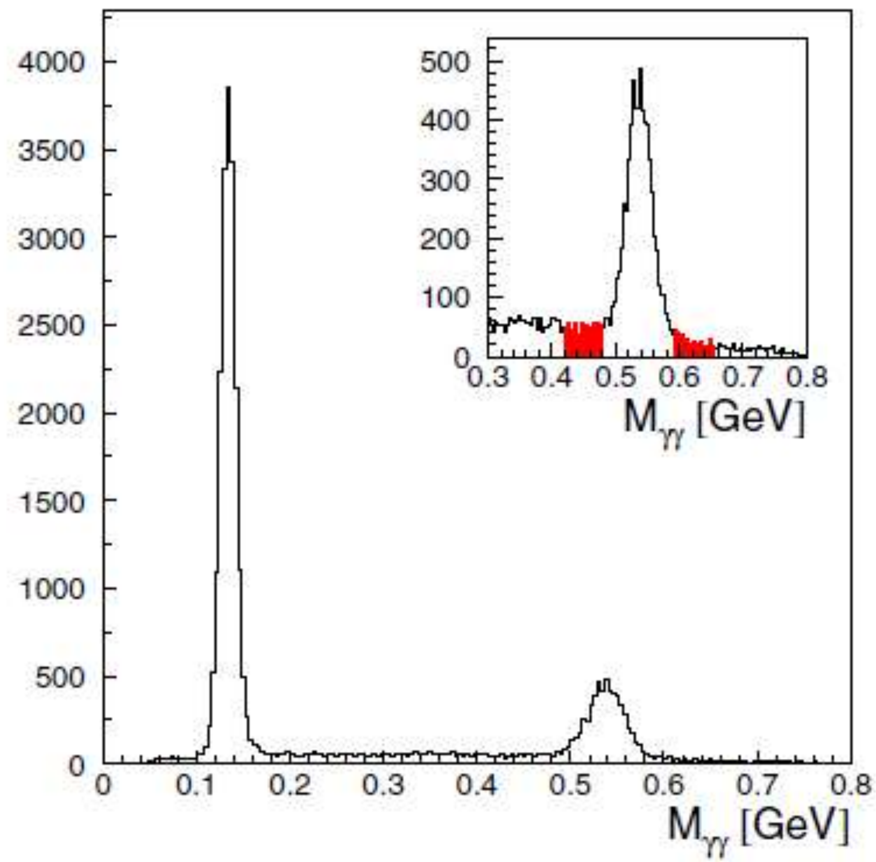

FIG. 8. The two-photon invariant-mass distribution $M_{\gamma\gamma}$ after all exclusivity cuts have been applied, for the case where the two photons are detected by the IC. The large peak at lower $M_{\gamma\gamma}$ is due to π^0 electroproduction and the smaller peak at higher $M_{\gamma\gamma}$ is due to η electroproduction. The inset magnifies the region around the η peak. The filled regions above and below the peak (red online) are the sidebands that are used for background subtraction, as discussed in the text.

Large-angle electromagnetic calorimeter ECAL0

ϕ-dependence of acceptance

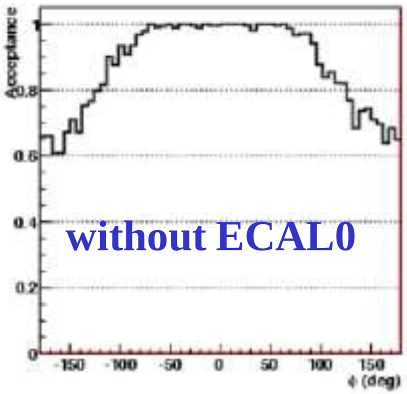

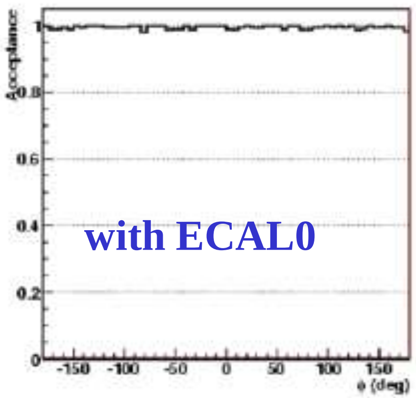

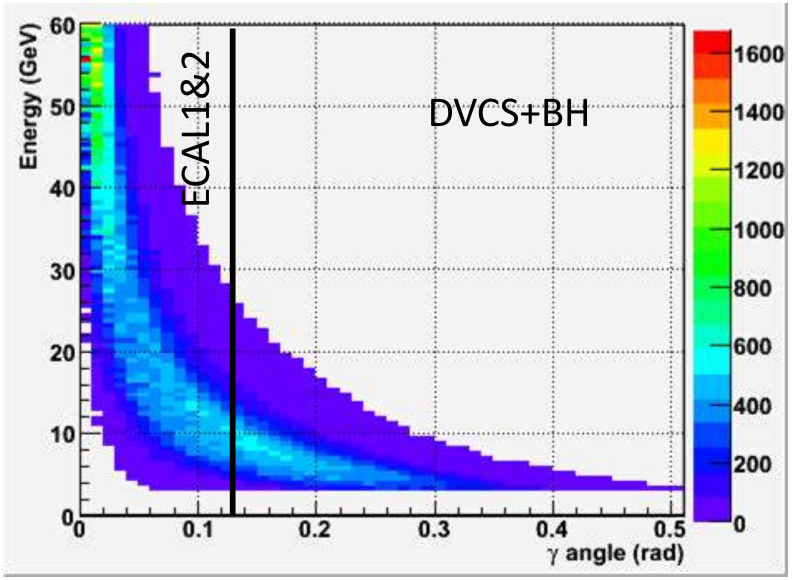

$Q^2 = 1.5 \pm 0.5\ (\text{GeV/c})^2$ and $x_{Bj} = 0.06 \pm 0.005$

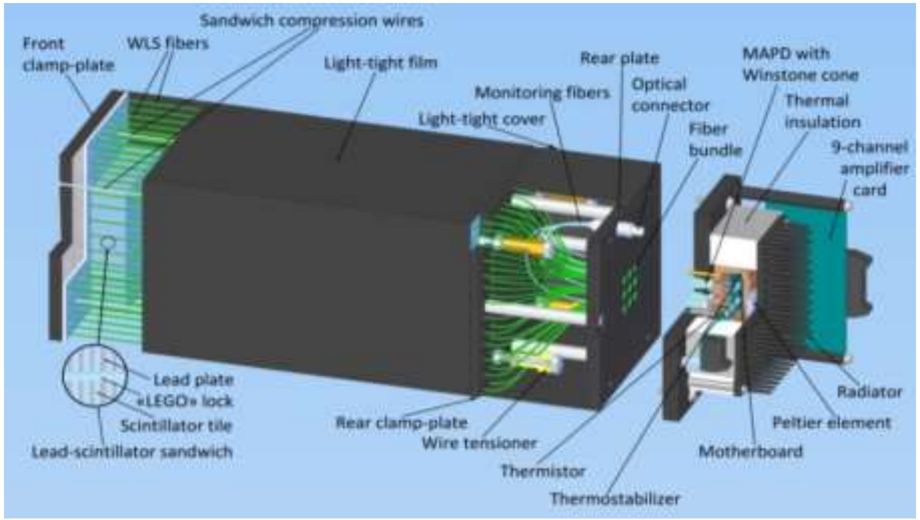

3D picture of proton via GPD

D. Mueller, X. Ji, A. Radyushkin, A. Belitsky, …
M. Burkardt, … Interpretation in impact parameter space

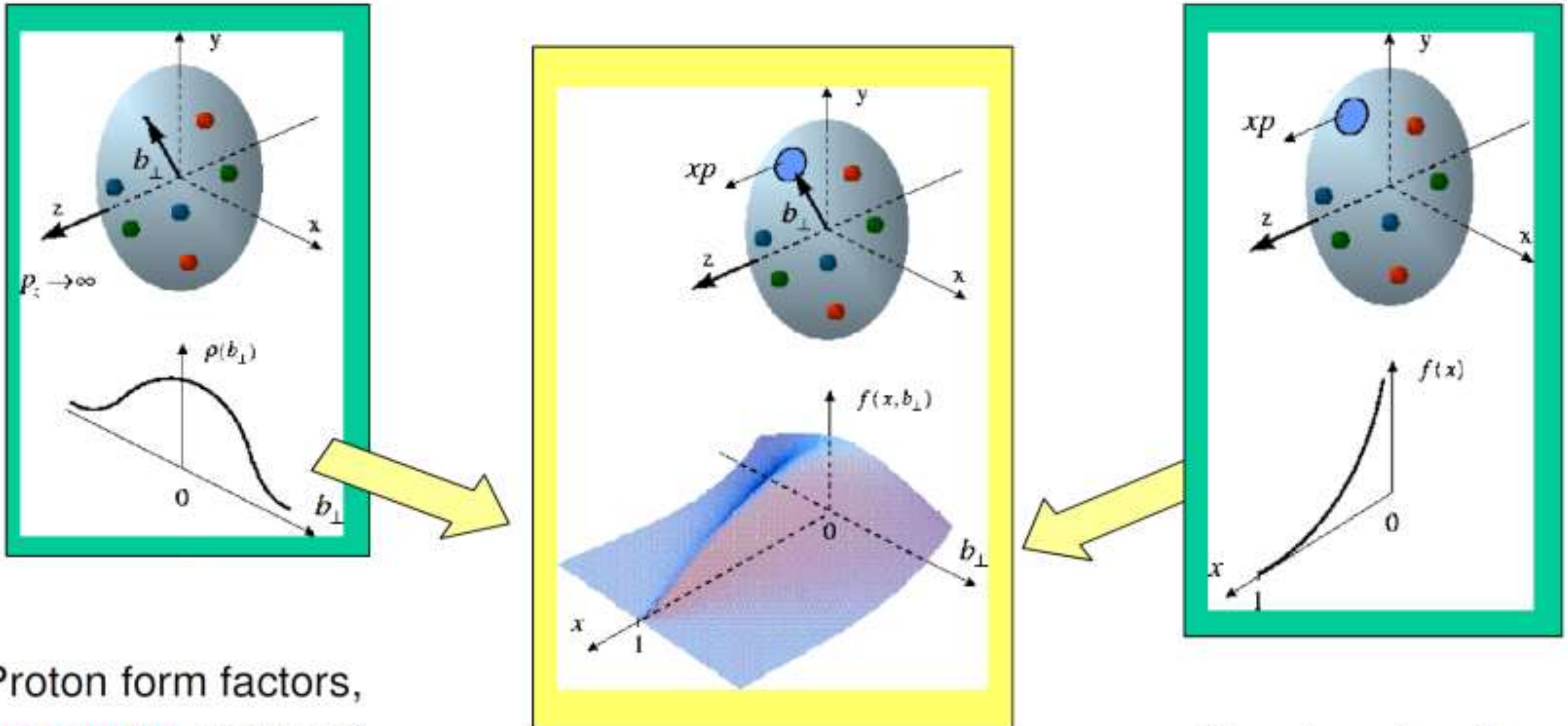

Proton form factors, transverse charge & current densities

Correlated quark momentum and helicity distributions in transverse space - GPDs

Structure functions, quark longitudinal momentum & helicity distributions

GPDs (x, b_T) TMDs (x, k_T)

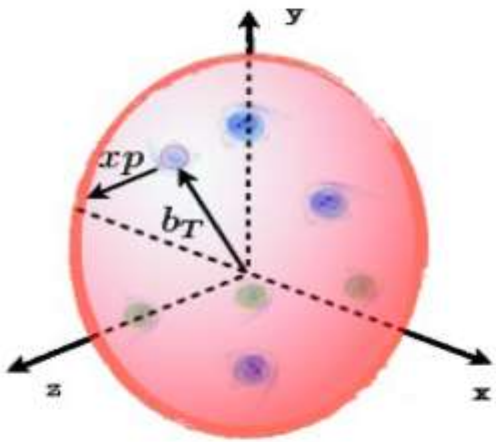

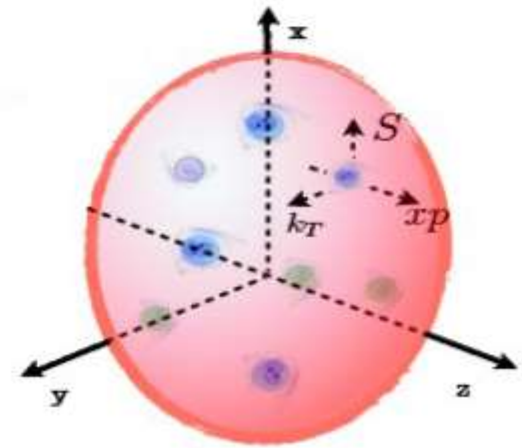

	GPD		TMD	
$\gamma^*_L\, p^{\uparrow} \rightarrow \rho_L\, p^{\uparrow}$	H	<=>	q (PDF)	
$\gamma^*_L\, p^{\uparrow} \rightarrow \rho_L\, p^{\downarrow}$	E	<=>	$f_{1T}^{\perp}$	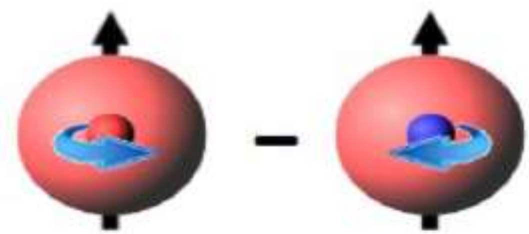
	Nucleon spin flip		**Sivers** Quark k_T, Transversely pol. nucleon	

2015

GPDs and Deep Virtual Exclusive Meson Production

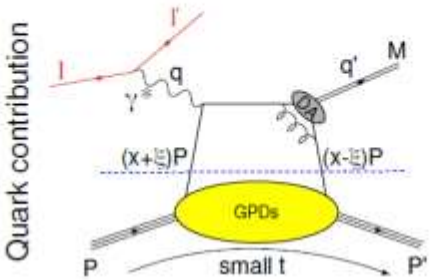

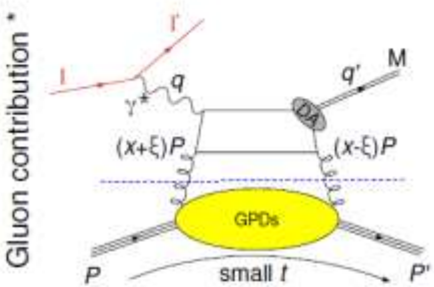

Chiral-even GPDs
helicity of parton conserved

$H^{q,g}(x,\xi,t)$ $\widetilde{H}^{q,g}(x,\xi,t)$	$E^{q,g}(x,\xi,t)$ $\widetilde{E}^{q,g}(x,\xi,t)$

Chiral-odd GPDs
helicity of parton flipped

$H^q_T(x,\xi,t)$ $\widetilde{H}^q_T(x,\xi,t)$	$E^q_T(x,\xi,t)$ $\widetilde{E}^q_T(x,\xi,t)$

Flavour separation
constraints for parton specific GPDs
due to different partonic content of mesons

Definition of variables:
q . . . γ^* four-momentum
x . . . average longitudinal momentum fraction of initial and final parton (NOT accessible)
ξ . . . difference of longitudinal-momentum fraction between initial and final parton $\approx x_B/(2-x_B)$
t . . . four-momentum transfer

* Gluon contribution at same order of α_s as from quarks

In general, hard exclusive π^0 is sensitive to the GPDs conserving the parton helicity $(\tilde{H},\ \tilde{E})$ and also to the parton helicity flip or to chiral-odd GPDs $(H_T \text{ and } \overline{E}_T)$, where $\overline{E}_T = 2\widetilde{H}_T + E_T$

Exclusive π^0 production: COMPASS acceptance ϕ averaged

4D acceptance in bins of ϕ_{π^0}, ν, $|t|$, Q^2
figure shows 3D projection, as a function of $|t|$